ACS OMEGA

http://pubs.acs.org/journal/acsodf

Review

Lithium Sulfide Batteries: Addressing the Kinetic Barriers and High First Charge Overpotential

Lewis Kien Juen Ting,[‖] Yulin Gao,[‖] Haimei Wang, Tuo Wang, Jianguo Sun,* and John Wang*

Cite This: *ACS Omega* 2022, 7, 40682−40700

Read Online

ACCESS | Metrics & More | Article Recommendations

ABSTRACT: Ever-rising global energy demands and the desperate need for green energy inevitably require next-generation energy storage systems. Lithium−sulfur (Li−S) batteries are a promising candidate as their conversion redox reaction offers superior high energy capacity and lower costs as compared to current intercalation type lithium-ion technology. Li_2S with a prelithiated cathode can, in principle, capture the high capacity while reducing some of the issues in conventional Li−S cells utilizing metallic lithium anodes and elemental sulfur cathodes. However, it also faces its own set of technical issues, including the insulating nature and the notorious shuttling effect that plagues the Li−S system. In addition, the high activation potential also hinders its electrochemical performance. To lower the high conversion barrier, key parameters of charge/ion transfer kinetics have to be considered in improving the reaction kinetics. This Review of lithium sulfide batteries examines the recent progress in this rapidly growing field, beginning with the revisiting of the fundamentals, working principles, and challenges of the Li−S system as well as the Li_2S cathode. The strategies adopted and methods that have been devised to overcome these issues are discussed in detail, by focusing on the synthesis of the nanoparticles, the structuring of the functional matrixes, and the promoting of the reaction kinetics through additives, aiming at providing a broad view of paths that can lead to a market viable Li_2S cathode in the near future.

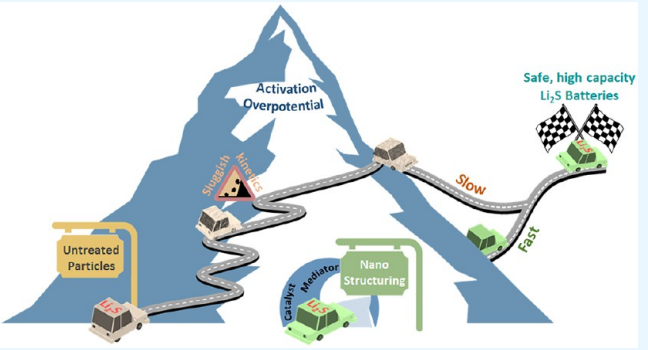

1. INTRODUCTION

The excessive consumption of nonrenewable energy has witnessed the adverse effects of climate change that impacts the environment, including global warming. To reduce the emissions of greenhouse gases, there is an urgent need to reduce the reliance on hydrocarbon fuels and electrify major polluting industries, such as manufacturing and transport. This evitable transition to renewable energy sources and the use of clean electricity in the widening range of applications demand for efficient and low-cost energy storage systems with high capacity and reliability.[1] Lithium-ion battery (LIB) technology has taken the market by storm over the past two decades, as the industry is able to scale its research and production along with the wide adoption of consumer electronics. However, LIBs have reached their theoretical limits, as they are apparently not viable for wider use in heavy industry. First, their maximum capacity is limited by a relatively low theoretical limit, making them unsuitable for applications that traditionally use a large amount of hydrocarbon fuels; second, their production relies heavily on costly transition metals such as cobalt and nickel, in addition to lithium, making their widespread adoption expensive and unsustainable.[2]

For the beyond LIB era, extensive exploration has been done to find safer, more reliable, and high capacity next generation energy storage technologies such as supercapacitors[3,4] and alternative ion batteries.[5] Among the various candidates, lithium−sulfur batteries (LSBs) have been under focused attention in recent decades for their multiple merits. The high specific capacity (1675 mAh g^{-1}) of sulfur is unparalleled by existing cathodes, allowing for high energy density storage. Furthermore, sulfur comes at a cheap monetary cost, due to its high abundance from mining and large-scale production. Additionally, it also provides value in the waste treatment of byproducts such as H_2S and SO_2 gas from other industrial activities, lowering the environmental costs. However, LSBs also come with multiple unsolved issues including the dendritic growth on metallic lithium, the large volume expansion of sulfur during charge/discharge, the low conductivity of both the S and the Li_2S discharge product, and the notorious shuttle effect of intermediate lithium polysulfides. In combination,

Received: August 25, 2022
Accepted: October 10, 2022
Published: October 31, 2022

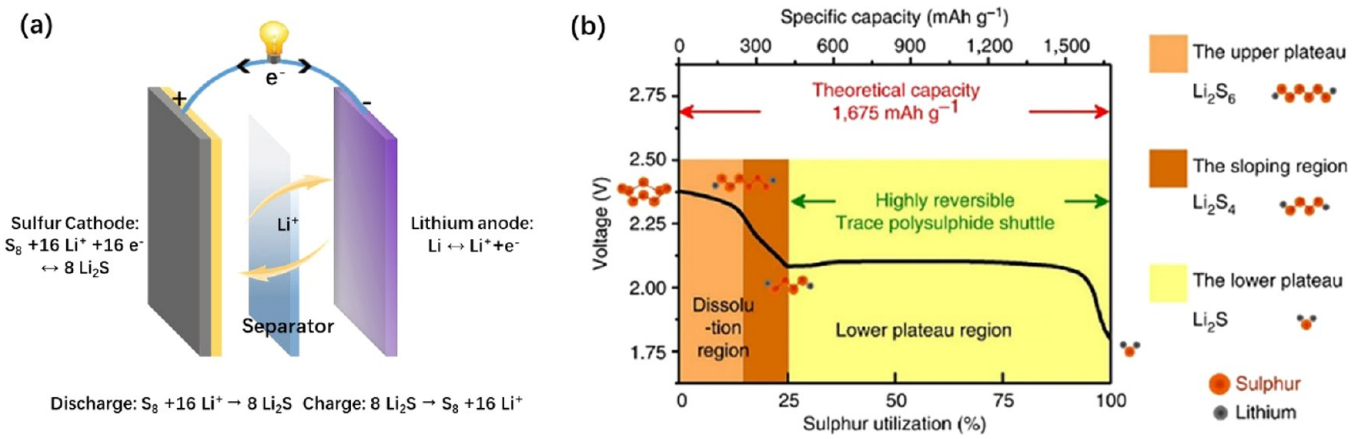

Figure 1. (a) Li−S battery system conversion reaction. Adapted with permission from ref 6. Copyright 2021 John Wiley & Sons, Inc. (b) Discharge profile of lithium sulfur battery (voltage vs specific capacity) and the reaction paths. Adapted with permission from ref 7. Copyright 2013 Springer Nature Limited.

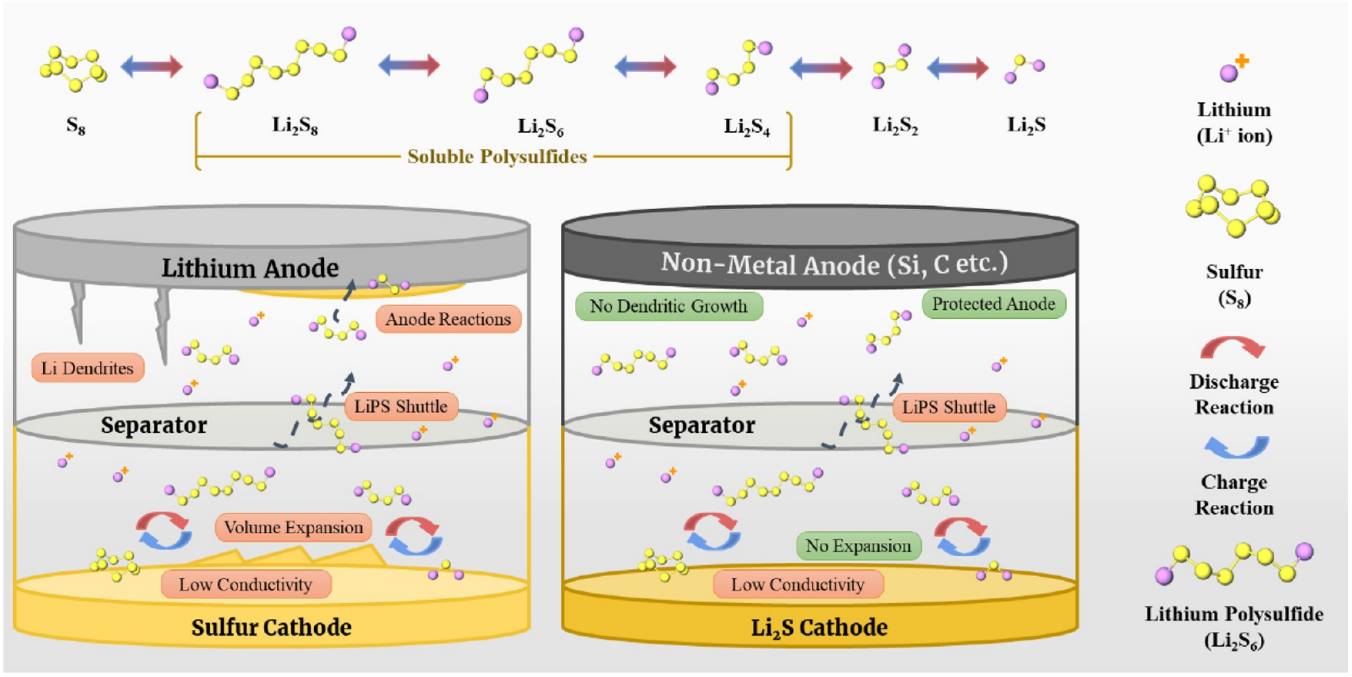

Figure 2. Illustration of the S_8 to Li_2S reaction and the challenges faced by the sulfur (S_8) and lithium sulfide (Li_2S) batteries.

these compromise the capacity, cyclability, and safety of the LSBs.

In the face of these challenges, research interest has grown in lithium sulfide (Li_2S)-based cathodes instead. Utilizing the lithiated form of sulfur offers several benefits, including allowing for the use of nonmetallic lithium anodes, stabilizing the volume expansion of the cathode, as well as a broader range of processing methods or operation environments enabled by its substantially higher melting point. These properties can address several challenges associated with both electrodes while retaining the superior energy capacity offered by the lithium sulfur (Li−S) battery system. Nonetheless, a key challenge of Li_2S cathodes is the high first charge overpotential, which must be addressed in practical batteries. As such, in this Review, we begin with an introduction to the Li−S battery system, followed by a comparison of S and Li_2S cathodes and the kinetic issues faced by Li_2S. Next, the various strategies that have been adopted to tackle the high first charge overpotential will be examined, along with their effects on the cell performance as a whole. Finally, we will propose some future directions of Li_2S cathode development for improved Li−S practical performance.

2. FUNDAMENTALS AND CHALLENGES IN LSBs

The high capacity of LSBs arises from two factors. At the anode, lithium provides both the highest theoretical specific capacity (3860 mAh g^{-1}) and the lowest redox potential (−3.04 V vs SHE)[8] among all known anode materials. At the other side of the electrolyte, the high charge and low mass of the S^{2-} ion likewise lead to one of the highest theoretical specific capacities (1675 mAh g^{-1}) among all known cathode materials.[2] Figure 1a illustrates the conversion reactions that occur at the electrodes in a typical lithium−sulfur system.[6] During the discharging process, the lithium anode will be ionized, and the resultant lithium ions migrate to the cathode, reacting with the sulfur cathode to form Li_2S, while the

https://doi.org/10.1021/acsomega.2c05477
ACS Omega 2022, 7, 40682−40700

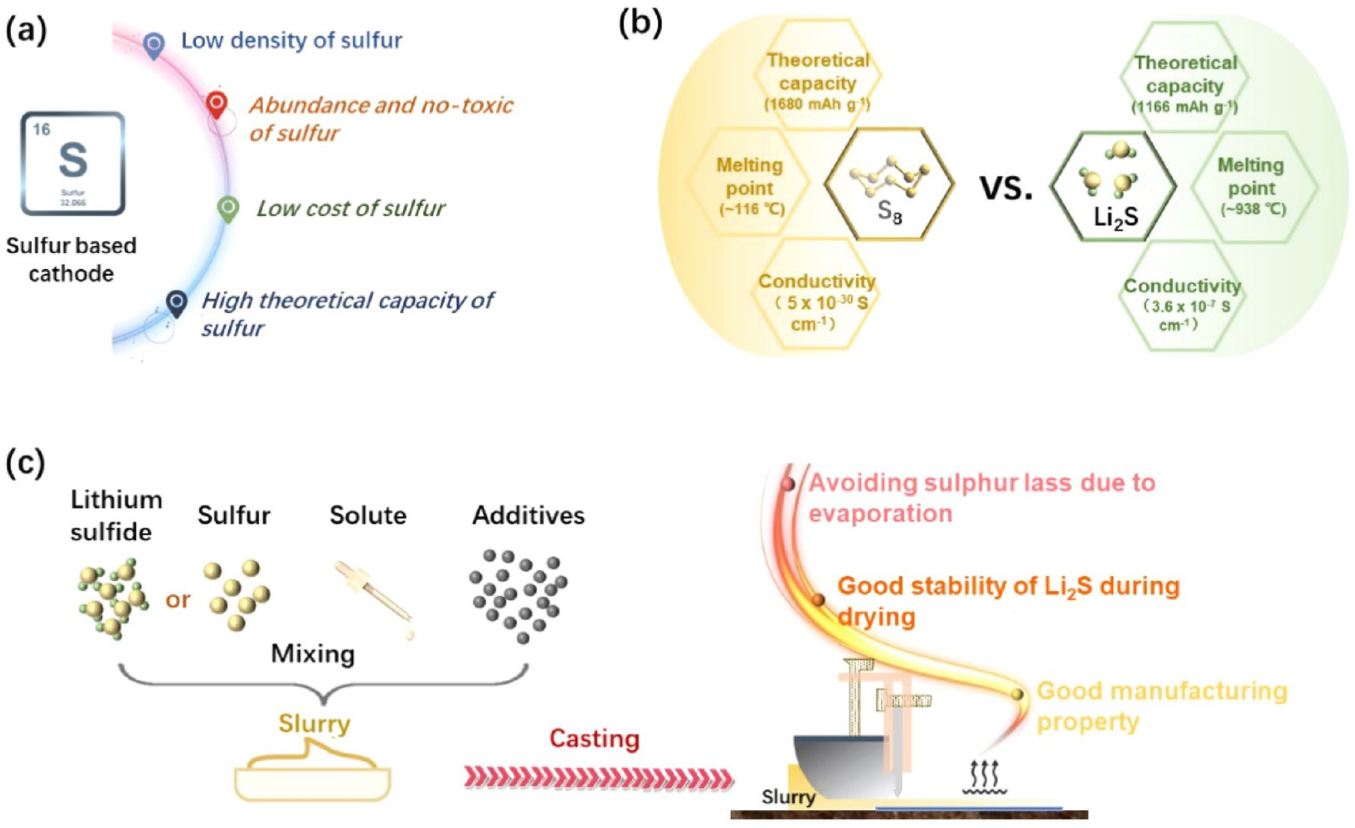

Figure 3. (a) Advantages of the sulfur chemistry, (b) comparison of the key metrics of sulfur and lithium sulfide, and (c) illustration of a typical slurry-based sulfur cathode preparation process and the advantages of using lithium sulfide instead of sulfur.

electrons generate a current through the external load. This process is reversed during the charging process: Li_2S is broken back down into elemental sulfur, which regenerates the cathode, while the lithium ions migrate back to the anode and combine with electrons, forming metallic lithium. However, the actual reaction between sulfur and lithium is rather complex. Typically, the conversion reaction during discharge at the sulfur cathode follows a progressive "solid−liquid−solid" transition process ($S_8 \rightarrow Li_2S_8 \rightarrow Li_2S_6 \rightarrow Li_2S_4 \rightarrow Li_2S_2 \rightarrow Li_2S$) as shown in Figure 1b.[9] The transformation is accompanied by two distinct plateaus that can be observed in the discharge profile.[7] The first plateau lies at around 2.3 V, corresponding to the reduction of sulfur from S_8 to long-chain Li_2S_n ($6 \leq n \leq 8$).[10] Following on, a sloping region appears and corresponds to the reduction of sulfur to short-chain Li_2S_4. These LiPSs are highly soluble in commonly used organic electrolytes, such as dioxolane (DOL) and dimethoxy ethane (DME). The first plateau and the sloping region together make up 25% of the theoretical capacity of sulfur. Afterward, the LiPSs will be reduced to solid Li_2S_2 and Li_2S at the lower plateau at 2.1 V, which are responsible for the remaining 75% of the theoretical capacity in the system.[6,11] However, during the charging process, the system does not display similar distinct two-plateau characteristics in the reverse reaction of converting Li_2S back into sulfur. Only a single broader peak, spanning a larger voltage range, appears and corresponds to a continuous oxidation process of LiPS species with no clear separation of phases, which can well be caused by the variety of multistep reactions with different activation energy barriers.

Despite the numerous advantages of LSBs, such as low cost, high capacity, and environmental friendliness (Figure 3a), commercialization has thus far been unsuccessful due to several challenges, as illustrated in Figure 2. First, lithiation of sulfur to Li_2S is accompanied by a large volume expansion of 80%, which can lead to pulverization of the sulfur particles as well as the cathode host.[12] Continuous pulverization will disrupt the electrode's integrity and induce fast capacity fading, which is even more serious in LSBs with high sulfur loading. Although this can be mitigated by utilizing porous matrixes that buffer the large volume expansion, doing so requires careful cathode design to ensure sufficient sulfur loading for optimal energy storage capability.[13] Another challenge is the low electronic and ionic conductivity of both S and Li_2S, leading to technical issues such as heightened internal resistance and poor reaction kinetics. The insulating reaction products may coat the exterior of the active material, inhibiting further redox reactions of the inner bulk. This results in low sulfur utilization and lowers the effective capacity of the electrode. To maintain an effective use of active material and high reaction efficiency, the sulfur loading is limited by its distance to reacting or conducting interfaces or requires the addition of conductive additives, both of which also limit the energy density of the cathode.[14] Furthermore, although the formation of soluble LiPS intermediates can improve the redox kinetics by enhancing ion transfer in the insulating Li_2S, it also poses the issue of dissolution and shuttle.[15] Specifically, LiPS shuttle is the phenomenon where the concentration gradient of soluble LiPS species in the electrolyte results in diffusion away from the cathode, through the separator, and to the anode.[14,16−18] The shuttled LiPS at the anode can react irreversibly with the lithium ions present to form an insulating lithium sulfide solid-electrolyte interphase (SEI), simultane-

https://doi.org/10.1021/acsomega.2c05477
ACS Omega 2022, 7, 40682−40700

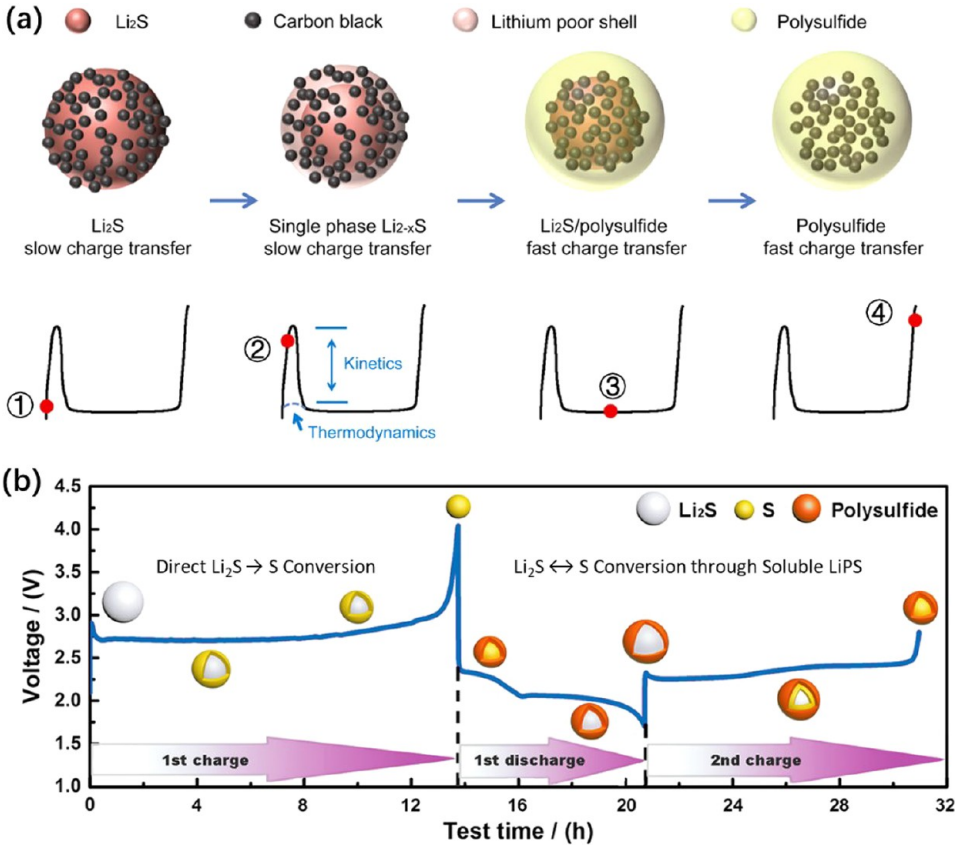

Figure 4. (a) Schematic of the first charge process in a Li_2S cathode, showing a high initial kinetic barrier due to slow charge transfer, followed by the lowered charge potential after the formation of soluble LiPS. Adapted with permission from ref 15. Copyright 2012 American Chemical Society. (b) Schematic showing the direct solid−solid conversion of Li_2S to S throughout the first charge process in a Li_2S cathode, resulting in high charge potentials, followed by polysulfide-mediated conversion in subsequent cycles, resulting in lowered charge potentials. Adapted with permission from ref 27. Copyright 2017 American Chemical Society.

ously depleting the active material and causing deterioration to the anode.[19]

In addition to the above challenges rising from the sulfur cathode, the lithium metal anode also suffers from nonuniform deposition-induced dendrites during the charging process.[20] Although morphologies such as moss-like and granular deposition can be benign in LSBs, dendritic (needle structured) lithium surfaces will form quickly with the increase of current density.[11] These dendrites can potentially break away from the electrode and become inactive "dead lithium" in the battery. They can also penetrate the separator, leading to internal short circuits that pose severe safety issues in practical applications.

3. LITHIUM SULFIDE BATTERIES: FROM SULFUR TO LITHIUM SULFIDE CATHODES

In addition to the aforementioned challenges, sulfur cathodes also face some difficulties with synthesis due to the physical properties of sulfur. Although sulfur is stable in air, common methods of producing sulfur cathode as illustrated in Figure 3c necessitate the use of raised temperatures and/or vacuum drying processes, which can easily cause the vaporization and loss of sulfur due to its low melting point. This impacts the true sulfur loading in the cathode and its practically available capacity and introduces uncertainties in experiments and the investigation process. Lithium sulfide as a cathode material has thus been explored instead. Utilizing the same chemical reaction between lithium and sulfur, we are still able to achieve a high theoretical specific capacity (1166 mAh g^{-1}). Although it is a step backward in capacity, it brings the apparent benefit of eliminating some issues posed by a common standard Li−S cell, as shown in Figures 2 and 3b. First, Li_2S has a much higher melting point (~938 °C) than does elemental sulfur (~116 °C), allowing for manufacturing and modification methods that involve higher temperature mechanical or chemical processes, and it also ensures the stability of such modifications of the Li_2S cell. At the same time, there will be less volume expansion issues during cycling, as the Li_2S cathode is synthesized in its fully lithiated form with the largest volume in the Li−S system. This eliminates the need for designed voids in the porous matrix or deliberate measurement of buffer material to cater for sulfur expansion. The structure of the cathode is thus reliant on the compressive rather than the tensile strength of the particulates, providing much better mechanical stability to the cathode, and alleviating cyclability and performance issues to some extent.[21] In addition, by using Li_2S as the cathode material, it effectively creates a system where lithium already exists in the cathode, which allows for the use of lithium metal-free anodes such as graphite,[22,23] silicon,[24] or tin,[25] to eliminate problematic dendritic growth and the formation of insulating Li_2S SEIs at the anode. In this case, utilizing the accumulation of LIB anode advancements over the decades would be ideal for the practical adoption of LSB. Meanwhile, it is worth noting that the safety issues that

https://doi.org/10.1021/acsomega.2c05477
ACS Omega 2022, 7, 40682−40700

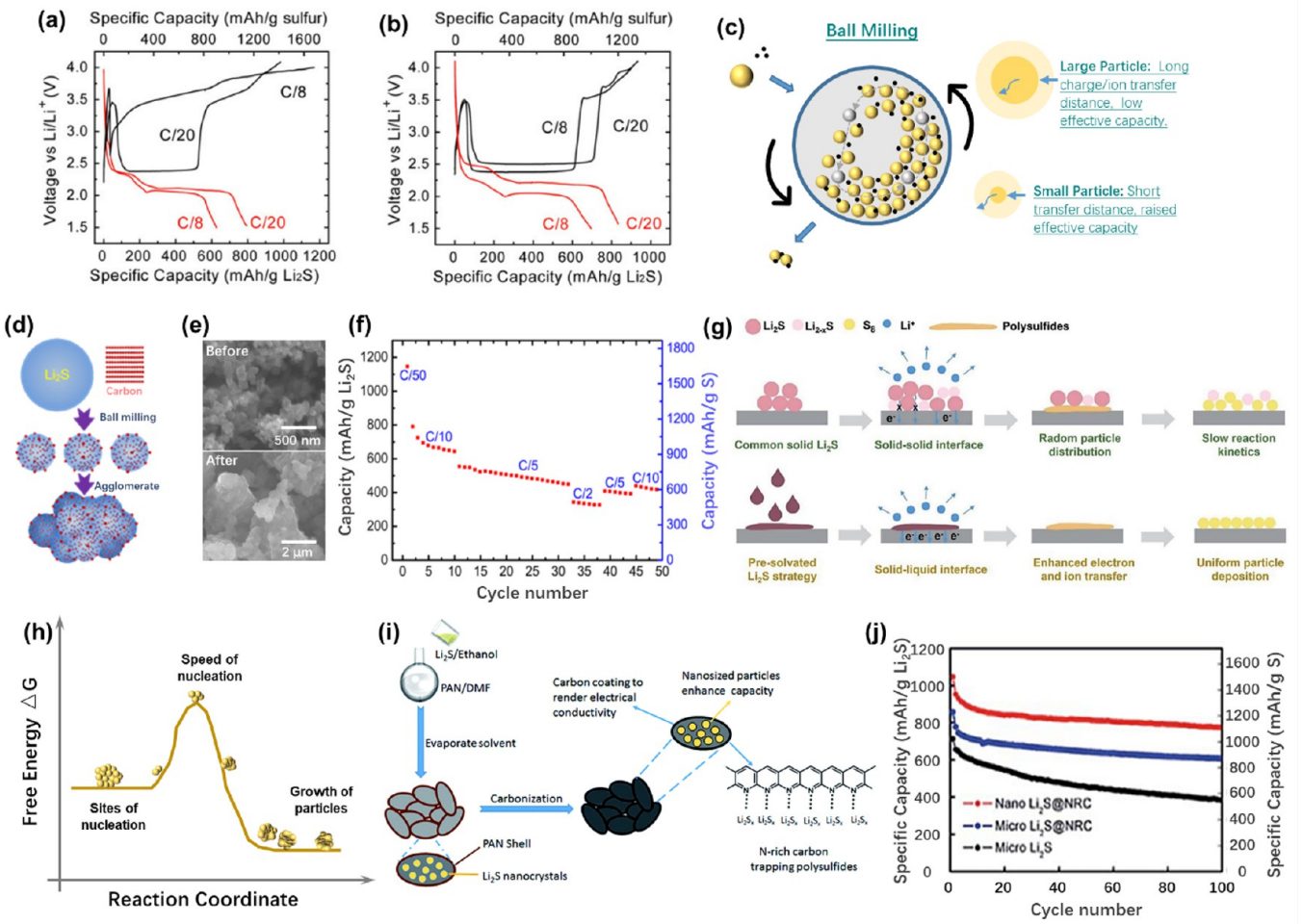

Figure 5. (a,b) Voltage profile of pristine (a) and ball-milled (b) Li_2S in the first cycle at C/20 and C/8. The voltage window is 1.5−4.1 V for C/20 and 1.5−4.0 V for C/8. The electrolyte was 1.0 M LiTFSI in DOL/DME without additive. The top axes in both (b) and (c) are based on the mass of sulfur in Li_2S. Adapted with permission from ref 15. Copyright 2012 American Chemical Society. (c) Effects of ball-milling and advantage of refining particle size and (d) schematic of the high-energy dry ball-milling process. (e) SEM image of commercial carbon black (Denka Black) powder and as-milled Li_2S−C composite agglomerates and (f) rate performance of the as-milled Li_2S−C composite cathode. Adapted with permission from ref 29. Copyright 2012 American Chemical Society. (g) Schematic diagram of electrochemical reaction processes in the solid Li_2S and preliquid Li_2S electrodes. Adapted with permission from ref 30. Copyright 2022 Royal Society of Chemistry. (h) Schematic illustration of nano-Li_2S@NRC composites, (i) schematic illustration of nano-Li_2S@NRC composites, and (j) cycling performances at 0.25 C. Adapted with permission from ref 31. Copyright 2016 Royal Society of Chemistry.

plagued early metal-anode LIBs can also be resolved in the metal-free anode system.[26]

However, one should note that, despite the differences in physical properties between sulfur and Li_2S, LSBs based on the Li_2S cathode still suffer from some similar issues to varying extents. Although the electrical conductivity of Li_2S is an order of magnitude higher than that of elemental sulfur, it is still very much an insulator that requires a conductive matrix or additives to function as a cathode. Furthermore, because the chemical reaction is the same as that of a pure sulfur cathode, the formation of soluble LiPSs and their shuttling effect is still an issue, albeit with better control over the formation of a passivating layer with the variety of anode choices.

In addition to these common challenges, Li_2S cathodes also face an activation issue, where studies have observed a high overpotential during the first charging process.[28] This overpotential then apparently disappears in subsequent charges, reverting to the typical charge profile of LSBs with pure sulfur cathodes. Such need of a huge overpotential for activation invites issues, such as decomposition of the electrolyte, which not only affects the electrochemical performance of the cell but also poses safety risks.[15] A detailed kinetic model for the activation of Li_2S activation was proposed by Yang et al. in 2012 (Figure 4a), who proposed that the high overpotential was associated with polysulfide nucleation around the Li_2S particle.[15] Because of the insulating nature of Li_2S, charge transfer in this initial stage between Li_2S, the electrolyte, and the conducting electrode additives was slow. A high charge potential of around 3.5 V is thus required to overcome this high charge transfer resistance. Once this initial barrier is overcome, the soluble LiPSs formed facilitate the rest of the conversion reaction by enhancing ion and charge transfer, allowing it to proceed at potentials much closer to the equilibrium potential of ∼2.5 V. This mechanism is supported by the disappearance of the overpotential upon the addition of PSs in the electrolyte.[15] However, Zhang et al. found direct transformation to sulfur in a solid−solid phase reaction without the involvement of LiPS species in the first charging process as shown in Figure 4b, where the high charge overpotential is instead attributed to breakage of the Li−S

https://doi.org/10.1021/acsomega.2c05477
ACS Omega 2022, 7, 40682−40700

Table 1. Summary of Studies on Reprocessed Li_2S and Cathode Performance

cathode content	Li_2S reprocessing method	particle size	current rate	specific capacity − Li_2S (mAh/g)	cycle number	capacity fade per cycle	first charge overpotential (V)
Li_2S-C-MWCNT[29]	ball-milled Li_2S	∼500 nm	C/10	1144	50	1.28%	3.7
Li_2S-CB[32]	ball-milled Li_2S	∼400 nm	C/2	640	100	0.61%	3.45
Li_2S-CB@N doped carbon			C/5	1029	100	0.37%	2.75
Li_2S-rGO paper[34]	ANH-EtOH Li_2S, drop-cast, vacuum-dried at 200 °C	25−50 nm	C/10	1119	150	0.18%	2.5
			C/2	898	145	0.16%	
			1C	752	145	0.12%	
Li_2S-MWCNT paper[35]	ANH-EtOH Li_2S, drop-cast, dried at 100 °C	7.8 nm	C/5	843	100	0.16%	2.48
			1C	729	100	0.13%	
Li_2S-CNF paper			C/5	827	80	0.17%	
nano-Li_2S@N rich carbon[31]	ANH-EtOH Li_2S, DMF displaced PAN cover and carbonized	<5 nm	C/2	1046	1000	0.041%	2.5
micro-Li_2S@N rich carbon		∼8 μm	C/4	853	100	0.35%	2.68
Li_2S-C@CVD[37]	ANH-EtOH Li_2S, evaporated polymer cover and carbonized	∼10 nm	C/2	780	250	0.09%	
Li_2S-C@CVD carbon shell			C/2	720	600	0.01%	
unprocessed Li_2S-C[38]	ANH-EtOH Li_2S, evaporated PVP cover and carbonized		C/5	920	100	0.10%	3.2
nanocomposite Li_2S@C		5−20 nm	C/5	472			3.7

bond.[27] Nonetheless, they agree with the view that soluble LiPSs formed during the discharging process are able to aid in reducing the overpotential after the first charge, in the fashion described by Yang's model.

Hence, to lower the first charge overpotential, these two factors of high charge transfer resistance and Li_2S conversion energy barrier must be addressed. Common strategies to target these factors involve lowering of the practical resistance in the electrode by reducing the charge transfer distance by refining the Li_2S particles, and the introduction of functional elements that catalyze the reaction, respectively. The methods used to achieve these will be discussed in detail in the following sections.

4. IMPROVEMENT STRATEGIES FOR LITHIUM SULFIDE BATTERIES

4.1. Structure Design: Synthesis Process and Substrates. *4.1.1. Reprocessing of Commercial Li_2S.* Commercially available Li_2S powders typically exhibit a particle size between 10 and 30 μm. Because of their insulating nature, a large portion of the particles' inner volume is prevented from sulfur conversion during charging cycles, thus reducing the capacity while displaying a high potential barrier to the conversion reaction. The low ionic conductivity also contributes to the high activation barrier during the first charge as shown in Figure 5a,b. By drastically reducing the particle size to the nanoscale, this insulating barrier can be overcome with the shortened diffusion length and enlarged contact surfaces (Figure 5c).[29] Various methods have thus been explored to refine readily available Li_2S for the high-performance LSB cathodes.

Ball-milling (Figure 5c) is a low-cost physical method to refine commercially available materials, capable of reaching the submicrometer scale within 100−500 nm,[15,29,32,33] and allows a thorough mixture of conductive additives concurrently. For example, Cai et al. have shown that the reduction in Li_2S particle size achieved through ball-milling is able to achieve nearly the full theoretical capacity of Li_2S, indicating full conversion to sulfur (Figure 5d−f). The first charge overpotential was also decreased by up to 0.2 V as compared to its bulk counterpart.[29] Nonetheless, ball-milling still has several apparent shortcomings. It is a physical, brute-force method of particle size refinement that is typically unable to produce particles smaller than 100 nm, which is insufficient for fully eliminating the first charge overpotential. In addition, ball-milled powders are prone to particle agglomeration, as shown by an example in Figure 5e,f, leading to long diffusion lengths despite apparently small particle sizes. Both effects would limit the benefits of ball-milling on the reaction kinetics, the first charge overpotential, and sulfur utilization.[29,32]

A chemical alternative is to reconstitute Li_2S through an intermediate liquid phase, also known as the presolvation method, as illustrated in Figure 5g. This utilizes the solubility of Li_2S in certain solvents such as ethanol, and the high volatility of such solvents. By dissolving Li_2S and evaporating the solvent, the oversaturation leads to precipitation of Li_2S. The method is capable of producing Li_2S particles as small as 5 nm, minimizing the diffusion length from the particle surface to its inner bulk and maximizing the associated benefits. Studies have been conducted to control the environment in which the process is made to take place to produce the desired size and morphology, including controlling the nucleation sites and the speed of nucleation and growth (Figure 5h). The knob of nucleation speed can thus be turned by manipulating the amount of solvent and its solubility. Solvents such as ethanol can easily be evaporated under the appropriate heat and vacuum, where the rate of solvent evaporation is controlled by the pressure and temperature. Wang et al. produced Li_2S particles of 25−50 nm on reduced graphene oxide (rGO) paper through this method by evaporating Li_2S−ethanol solution at 300 °C, with the resultant cathodes displaying a substantially lowered first-charge potential of 2.4 V.[34] Wu et al. similarly used evaporation of the Li_2S−ethanol solution, but at 100 °C in low vacuum, resulting in particles of sub-10 nm in sizes in the pores of multiwalled carbon nanotubes (MWCNT) paper, which showed a first charge potential of as low as 2.2 V, virtually eliminating the overpotential.[35] Other than directly evaporating the solvent, studies also explored altering the

https://doi.org/10.1021/acsomega.2c05477
ACS Omega 2022, 7, 40682−40700

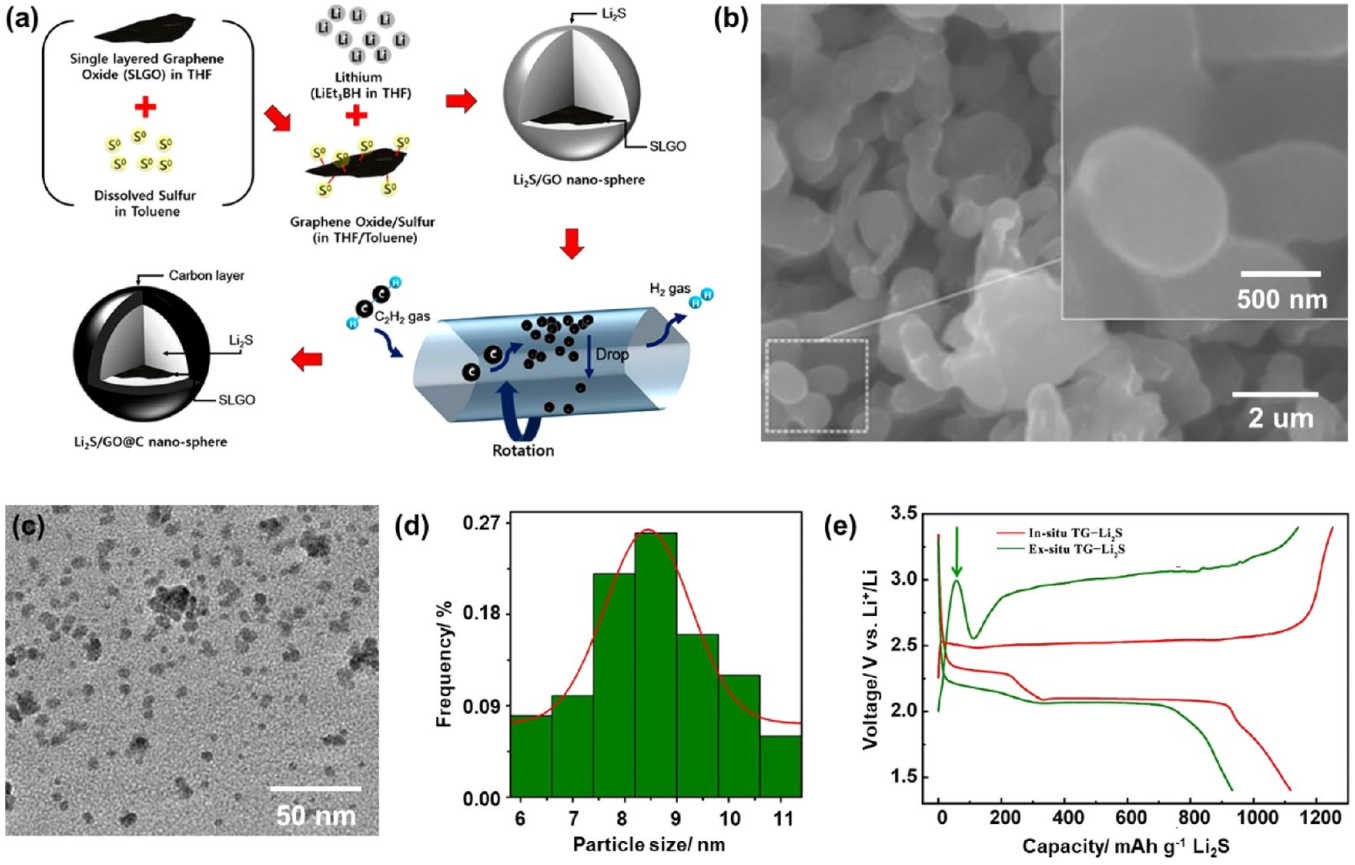

Figure 6. (a) Illustration of the nanoparticle synthesis process by sulfur presolvation in toluene and lithiation with $LiEt_3BH$ and (b) the resultant Li_2S nanoparticles. Adapted with permission from ref 39. Copyright 2015 American Chemical Society. Li_2S synthesized via infiltration of graphene nanosheets with molten sulfur followed by lithiation with $LiEt_3BH$, showing (c,d) an ultrasmall particle size and (e) a substantially lowered first charge potential as compared to commercial (ex situ) Li_2S. Adapted with permission from ref 41. Copyright 2014 Springer Nature Limited.

solubility by introducing solvents miscible with ethanol, but with lower Li_2S solubility such as DMF. Hu et al. have demonstrated the production of Li_2S nanocrystals of ∼5 nm in sizes by using the solvent exchange method, similarly displaying a high initial capacity utilization at 1046 mAh g^{-1} (Figure 5i,j), and reported virtually no first charge overpotential.[31]

The introduction of numerous nucleation sites is likewise important in reducing particle sizes. To induce suitable nucleation sites for Li_2S, web-like porous structures are commonly used due to the abundance of surface active sites for nucleation. At the same time, the separation of internal surfaces in these structures further prevents the agglomeration of newly grown particles. However, it is well-known that the growth in particle size is not easily halted by just stopping the evaporation of solvents, as coalescence and Ostwald ripening can still occur.[36] Additives such as polyvinylpyrrolidone (PVP), polyacrylonitrile (PAN), etc., can be introduced to form an encapsulating polymer layer, which stabilizes the Li_2S particles and prevents redissolution and/or steric interactions between particles.[31,37,38] Indeed, Wu et al. have produced Li_2S nanocrystals of 5−20 nm in clusters, sealed within PVP as they are formed by precipitation simultaneously from the evaporation of the solvent. The polymer is then carbonized at a high temperature of 700 °C under an argon environment, forming Li_2S/C composite powders that can operate at high sulfur utilization with a low first-charge overpotential of less than 3.0 V without the use of expensive materials such as rGO and MWCNTs.[38] Wu et al. also produced rather uniformly distributed Li_2S clusters of ∼10 nm in sizes, sealed within graphitic carbon using the same method, and further added with a hard carbon layer via CVD. The reinforced hierarchical structure demonstrated a high cycling stability and retention of up to 600 cycles, as compared to the ∼100 cycles in typical prior studies.[37] Such high temperature processes are viable by virtue of the Li_2S crystals' high melting temperature, allowing the particles to remain stable both during processing and also during operation, making high-temperature applications not only viable but also possibly desirable due to the elevated ionic conductivity.[38] Table 1 summarizes the methods used to reprocess commercial Li_2S and their resulting key performance parameters. It can be seen that nanostructuring of Li_2S can lead to a significant improvement in capacity utilization and reduction in overpotential, and while other improvement strategies may have potentially enhanced the cathode further, studies also show that the lack of particle refinement would always lead to suboptimal performance.

4.1.2. Direct Synthesis of Li_2S. While the efforts to reduce the first charge overpotential by reprocessing commercial Li_2S have been largely successful, Li_2S is highly sensitive to moisture, decomposing readily into LiOH, making it hard to store and transport. Thus, various methods to directly synthesize Li_2S from precursor chemicals that are relatively shelf-stable have been explored. These can be generally categorized into three paths on the basis of the precursor types: (1) lithiation of sulfur-rich nanoparticles, (2) sulfurizing

https://doi.org/10.1021/acsomega.2c05477
ACS Omega 2022, 7, 40682−40700

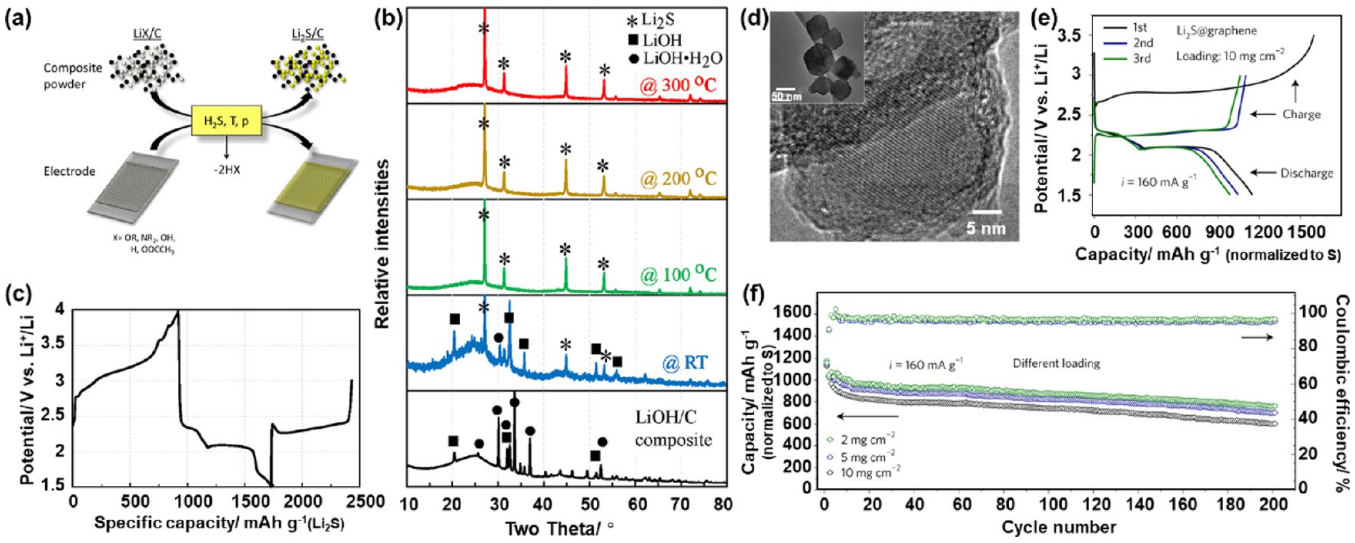

Figure 7. (a) Schematic of the synthesis of Li_2S from lithium salts and H_2S, with successful synthesis demonstrated using (b) XRD at different synthesis temperatures. The resultant cathode showed (c) typical Li_2S charge/discharge curves. Adapted with permission from ref 42. Copyright 2016 Elsevier. (d) TEM image of single crystal Li_2S encapsulated by graphite (inset: bulk nanocapsules), synthesized by burning lithium in CS_2, exhibiting (e) a first charge potential of less than 3 V and (f) excellent capacity and cycle stability, even at high sulfur loading. Adapted with permission from ref 45. Copyright 2017 Springer Nature Limited.

lithium-rich nanoparticles, and (3) synthesis from precursors that contain both lithium and sulfur. However, it is worth noting that, although the precursor materials are generally stable before synthesis, the end product of Li_2S requires an inert environment to prevent decomposition, and thus all processes are typically conducted in a controlled atmosphere.

4.1.2.1. Lithiating Sulfur-Rich Precursors. Unlike Li_2S, elemental sulfur is shelf stable, so it is therefore logical to first attempt to capitalize on sulfur to create either sulfur nanoparticles or sulfur cathode, followed by lithiation. In 2010, Yang et al. made use of the well-researched CMK-3 mesoporous carbon matrix, and infiltrated the pores with molten sulfur at 155 °C, where its viscosity is the lowest. This exploited the low melting point of sulfur and the good wettability of liquid sulfur on carbon, and the resultant sulfur cathode material was then lithiated with *n*-butyllithium.[40] Other chemicals such as lithium triethyl borohydride ($LiEt_3BH$) have been experimented with as well, as illustrated in Figure 6a. For example, Hwa et al. used toluene as a medium to dissolve sulfur and nucleate nanoparticles on single-layered GO (SLGO), which was then lithiated with $LiEt_3BH$. The resultant particles molded around the GO flakes were of 500−800 nm in size (Figure 6b), which were then carbon coated using CVD in a rotating furnace.[39] Most of these early studies were unable to generate particles of sub-100 nm size, with limited success in lowering the first charge potential. Zhang et al. produced Li_2S particles of ∼8.5 nm size by introducing molten sulfur in graphene nanosheets, which were then lithiated with $LiEt_3BH$ (Figure 6c,d). This was able to eliminate the first charge potential and achieve a high specific capacity of more than 1000 mAh g^{-1} (Figure 6e). However, this study still found serious agglomeration of Li_2S particles and also faced cycling stability issues, with severe capacity degradation within 100 cycles.[41]

These studies opened the possibility of further developing high-performance cathodes, as the highly stable particles could be generated by carbon coating through CVD, providing an excellent cycling performance of up to 1000 cycles as was demonstrated by Hwa et al.[39] However, the major drawbacks of these lithiating methods originated from the unstable lithium compounds used, which could be hazardous when exposed to moisture and oxygen. *n*-Butyllithium is pyrophoric, while $LiEt_3BH$ is highly flammable, and both are corrosive or can decompose to become corrosive. Their usage thus faces the same challenges as unstable Li_2S. As many lithium compounds tend to exhibit similar hazards and instability, alternative approaches of directly using stable lithium precursors have been explored.

4.1.2.2. Sulfurizing Lithium-Rich Precursors. Various lithium salts, such as LiOH, Li_2CO_3, and $LiNO_3$, are relatively stable in the ambient environment. Dressel et al. demonstrated the sulfurization of LiOH using H_2S with an inert environment being used only at the final step and pointed out the greatly reduced need of a controlled atmosphere throughout the fabrication process.[42] The following reaction was involved, which is also generalized to several strong Bronsted base LiX salts, where X = OH, NH_2, H, or CH_3CH_2O:

$$2LiOH\ (s) + H_2S\ (g) \rightarrow Li_2S\ (s) + 2H_2O\ (g)$$

$$2LiX\ (s) + H_2S\ (g) \rightarrow Li_2S\ (s) + 2HX\ (g)$$

The lithium salt can be processed with methods similar to those for handling commercial Li_2S, such as ball-milling to reduce their size or recrystallizing into nanoparticles. The particles can then be handled as needed to form composite material electrodes before being finally processed in a controlled atmosphere by heating with a constant flow of H_2S gas, as shown in Figure 7a. It was observed that the hydroxide, hydride, nitride, and ethoxide salts of lithium can be converted at least partially from 100 °C upward, while the acetate and carbonate salts require 350 and 400 °C, respectively, for the conversion to happen (Figure 7b). The resultant Li_2S cathode was able to exhibit a relatively high discharge capacity of 770 mAh g^{-1} with typical Li_2S charge/discharge curves (Figure 7c), demonstrating the viability of synthesizing high-performance Li_2S through air-stable lithium

https://doi.org/10.1021/acsomega.2c05477
ACS Omega 2022, 7, 40682−40700

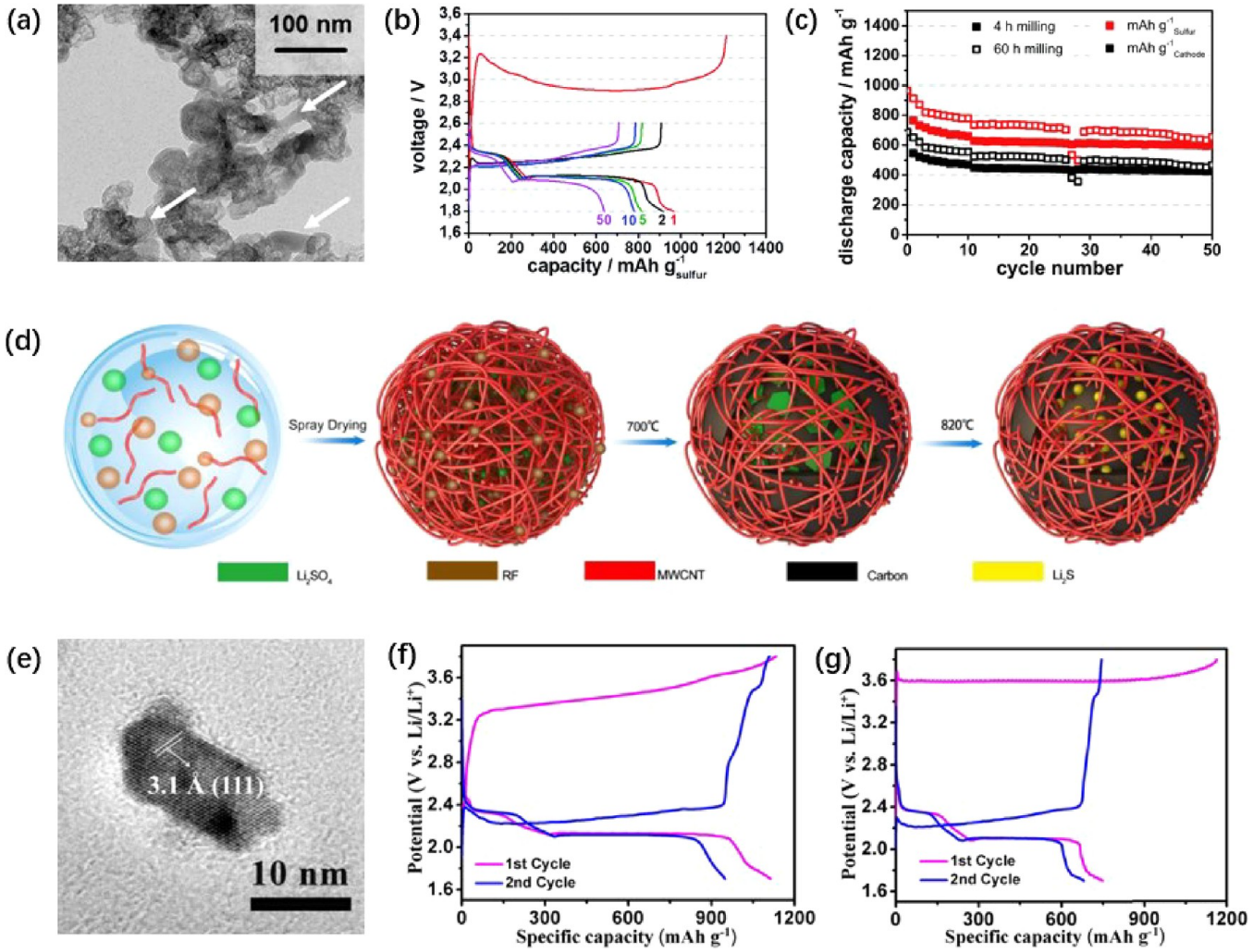

Figure 8. (a) Li_2S nanoparticles synthesized by carbothermal reduction of Li_2SO_4, showing (b) a lowered first charge overpotential and (c) good capacity and cycle stability. Adapted with permission from ref 51. Copyright 2015 Royal Society of Chemistry. (d) Schematic of the synthesis of Li_2S via dissolution and spray drying of Li_2SO_4, followed by the carbothermal reduction in the presence of resorcinol-formaldehyde and CNTs, forming (e) very small nanoparticles of around 10 nm. The small particle results in (f) a significantly reduced first charge overpotential and higher sulfur utilization as compared to 40 μm particles synthesized with (g) a similar method without CNT. Adapted with permission from ref 52. Copyright 2019 Elsevier.

salts.[42] Some other techniques for generating fine particulates that were not applicable due to the hazardous nature of precursor materials are also available with the use of air-stable lithium salts. For example, Hart et al. used aerosol spray pyrolysis of various lithium salt solutions with sucrose as a carbon source to obtain fine lithium carbonate particles, which were then sulfurized to obtain Li_2S at a high temperature of 725 °C. The particles were made into an electrode via the standard slurry method, however, yielding an unremarkable performance. Better performance is obtained from particles with lithium carbonate as the precursor, yielding Li_2S cathodes with the first charge overpotential of ~2.75 V and an initial capacity of 690 mAh g^{-1}, ~60% of the theoretical limit of Li_2S cathode.[43] Nava-Avendaño et al. studied the scalability of the reaction with H_2S by using thermal plasma with good success, where particles in the range of ~20 nm were produced by reacting LiOH precursors to produce electrode with fully suppressed first charge overpotential. However, the sulfur utilization was fairly low at 62% after cycling. This is also paired with a nontrivial amount of byproducts and unreacted precursor feed, complicating the reaction and demands' postprocessing.[44]

Lithium metal can also be used directly as the lithium source for reaction with H_2S, which trades generally more complete reactions at lower temperatures for the higher volatility and instability of lithium metal. Alcohol can be used as a mediator to lower the reaction potential with H_2S gas, allowing the complete reaction with a gaseous byproduct that is easily removed from the desired Li_2S product.[46] Zhao et al. used ethanol to carry out the synthesis at room temperature with a reaction route involving both liquid- and gas-phase reactions:

$$\mathrm{Li\ (s) + EtOH\ (l) \rightarrow LiOEt\ (l) + H_2\ (g)}$$

$$\mathrm{LiOEt\ (l) + H_2S\ (g) \rightarrow Li_2S\ (s) + EtOH\ (l)}$$

The method was able to produce Li_2S nanocrystals (NCs) of sub-10 nm sizes, where the annealed product, by simply using a standard slurry spread, was able to yield an initial capacity of up to 98.5% of Li_2S theoretical limit with no appearance of the first charge overpotential reported.[47] It is however also

https://doi.org/10.1021/acsomega.2c05477
ACS Omega 2022, 7, 40682−40700

noteworthy that the necessary annealing step to break down complexes formed with alcohol can give rise to the Ostwald ripening of Li_2S NCs, if conducted at an excess temperature, which has been shown to negatively affect electrode performance in terms of capacity utilization. The Li_2S NCs also proved to be unstable in cycling performance, quickly degrading to less than 50% of the initial capacity within 100 cycles.

An alternative synthesis route involves the use of CS_2 gas instead, with the goal of incorporating carbon as a conductive additive and protective coating into the produced particle in a one-step process with the reaction: $4Li(s) + CS_2(g) \rightarrow 2Li_2S(s) + C(s)$. This process faces the same issues as before, as lithium metal is unstable in atmosphere. Tan et al. produced Li_2S particles in the size range of 50−100 nm with a graphene coating layer by combustion of molten lithium metal at 650 °C as shown in Figure 7d. The resultant particles allowed a remarkable 95% delithiation in the first charging process, but still experienced a charge overpotential of 2.74 V, and only retained ∼70% of the initial capacity in the following discharge cycles, as shown in Figure 7e,f.[45] This method comes with an obvious hazard of handling molten lithium and a violent combustion reaction, but did not yield significantly improved results in comparison to methods with H_2S gas. Liang et al. produced Li_2S particles in the size range of 5−15 nm by a similar exothermic reaction between LiH/CNT mixture and CS_2 gas, with the initiation temperature lowered to 250 °C, albeit with an extra hydrogen gas byproduct. This method demonstrated significant improvement over previous studies, yielding a specific capacity of 87% of Li_2S theoretical limit, with no notable first charge overpotential being present.[48] However, the contribution from the CS_2 reaction for carbon addition remains debatable due to the introduction of CNT in the mixture, which has been shown to aid with nanoparticle formation and thus an improvement in performance in other studies.[35,38]

Progress has been made in utilizing the gas-phase sulfurization of lithium precursors, and methods have been developed to avoid violent combustion and high-temperature reactions to yield Li_2S cathodes of promising performance. However, the involvement of toxic gases, such as H_2S and CS_2, and the complex reactor designs along with the treatment of dangerous byproducts such as combustible H_2 gas still pose a high barrier to accessing these high-performance Li_2S nanoparticles through the gas-phase sulfurization route.

4.1.2.3. Bring Both from the Start. A more direct synthesis method utilizes stable precursors that contain both lithium and sulfur. Lithium sulfate (Li_2SO_4) is the sulfuric acid salt of lithium. While it is hygroscopic, it forms lithium sulfate monohydrate, which is relatively stable in atmospheric conditions, unlike the decomposition of Li_2S. Any crystalline water content can also be relatively easily removed by evaporation using heat treatment, and the salt itself can be converted into Li_2S through carbothermic reduction ($Li_2SO_4 + C \rightarrow Li_2S + CO_2/CO$).[49] The various forms of carbon sources available make the carbothermic reduction of lithium sulfate to Li_2S versatile, unlike the frequently unstable and corrosive lithium sources for lithiating sulfur, or the gaseous and toxic sulfur sources used to react with lithium precursors. Studies have verified the viability of various carbon sources, such as petroleum coke,[49] carbon black,[50] among others, with attempts to find the optimal processing temperature and carbon ratio for conversion to Li_2S. However, the final product heavily relies on the lithium sulfate feedstock to achieve submicrometer size for optimal cell performance, and the toolbox used to refine Li_2S can similarly be applied to lithium sulfate.

An obvious method of ball-milling allows refining lithium sulfate to ∼150 nm particle sizes, which can then be reduced by a carbothermic reaction. Indeed, Kohl et al. demonstrated that this allows conversion to lithium sulfide particles of 50−100 nm size as shown in Figure 8a. This results in electrodes with up to 80% capacity utilization as compared to the theoretical limit with good cycling stability, with a fairly high first charge overpotential of 3.2 V, as shown in Figure 8b,c.[51] While this is superior to that using the physical method to refine Li_2S as is, the size of which this method can yield is still limited, and problems mentioned above with ball-milling still persist. Furthermore, the carbothermic reaction requires high temperatures for an efficient conversion, while the need for small particles demands a lower reaction temperature to avoid agglomeration. These two requirements are in direct conflict and limit the effectiveness of the synthesis route through physical methods.

By making use of the solubility of lithium sulfate in water, the liquid-phase methods used on Li_2S become applicable as well, with the added benefits of lithium sulfate's stability under ambient conditions. The salt solution can be used to nucleate lithium sulfate nanoparticles with various methods that might be difficult or prohibitive in the case of Li_2S, such as spray drying,[52] freeze-drying,[53] and electrospinning.[54] Using resorcinol-formaldehyde (RF) as a carbon source, Chen et al. produced a solution of Li_2SO_4@RF particles attached to the dispersion of CNT, which was then spray dried to form granules of hierarchical structures as illustrated in Figure 8d,e. The carbothermal reduction of these granules can produce Li_2S particles of 10 nm in size, with agglomeration being prevented by the RF coating during the drying process.[52] The resulting electrode exhibited a high initial capacity at 94.3% of the theoretical limit and retained a reversible capacity of 642 mAh g^{-1} through cycling tests. However, although the small particle size reduced the first charge potential, it remained fairly high at 3.2 V.[52] Li et al. freeze-dried a lithium sulfate glucose solution onto bacterial cellulose (BC) hydrogel, and the resultant Li_2SO_4@glucose@BC structure was then pyrolyzed. The thermal process converts cellulose into carbon fibers and glucose into porous carbon, while lithium sulfate is reduced to Li_2S and deposited within the ∼5 nm pores in the PC@CNF frame. The one-step process produces a free-standing electrode, bypassing the need of slurry casting, with a reported reversible capacity at 500 mAh g^{-1} after 400 cycles and a 3.2 V first charge potential (Figure 8f,g).[53] Other than lithium sulfate, new air-stable precursors are being synthesized. Brune et al. used $(LiSC_2H_4)_2NMe$, a molecule stable under atmospheric conditions while soluble in polar solvents. It was used in combination with PVP to form 1D fibers loaded with the Li_2S precursor via electrospinning.[54] While following a different reaction, the molecule is similarly stripped of components other than the desired Li_2S through thermal treatment at 350 °C, leaving behind particles of ∼10 nm in size. This approach generated Li_2S cathode with a capacity of 702 mAh g^{-1} with a capacity retention of 73% after 100 cycles, but faced a high first charge activation barrier of 3.7 V.[54]

In brief summary, this section provided an overview of the studies conducted, and their directions in developing Li_2S cathode synthesis methods. Through initial studies using physical ball-milling methods, it was discovered that the high-performance Li_2S cathode requires the ability to synthesize

https://doi.org/10.1021/acsomega.2c05477
ACS Omega 2022, 7, 40682−40700

Table 2. Summary of Studies on Direct Synthesized Li_2S and Cathode Performance

cathode content	precursor and process	particle size	current rate	specific capacity – Li_2S (mAh/g)	cycle number	capacity fade per cycle	first charge overpotential
Li_2S-CMK-3 composite	molten sulfur, *n*-butyllithium[40]		C/8	573	20	1.95%	2.5 V
(in situ) Li_2S-TG composite	sulfur, $LiEt_3BH$[41]	~8.5 nm	C/10	1119	100	0.29%	negligible
(ex situ) Li_2S-TG composite			C/10	933	100	0.52%	3 V
Li_2S/GO	toluene dissolve sulfur, $LiEt_3BH$, CVD[39]	0.5–0.8 μm	C/5	740	50	0.85%	3.75 V
Li_2S/GO@C			C/5	964	50	0.42%	2.6 V
Li_2S/C	LiOH, H_2S[42]		C/5	770	100	0.47%	
Li_2S-C(Carb)	Li_2CO_3, $LiNO_3$, CH_3COOLi, sucrose, H_2S at 725 °C[43]	~500 nm	C/10	690	100	0.16%	2.75 V
Li_2S-C(Nit)		~0.8 μm	C/10	625	100	0.34%	2.8 V
Li_2S-C(Acet)		0.5–1.5 μm	C/10	650	100	0.11%	2.8 V
Li_2S(OH)	LiOH, Li_2SO_4, H_2S, CH_4 tube furnace at 800 °C[44]	N/A	N/A	N/A	N/A	N/A	3.5
Li_2S-C(SO_4)							3.7
plasma Li_2S(OH)	LiOH, Li_2SO_4, H_2S, CH_4 Ar plasma[44]	N/A	N/A	N/A	N/A	N/A	2.5
plasma Li_2S-C(OH)		~20 nm	C/10	610	10	5.90%	2.33
plasma Li_2S-C(SO_4)				520	10	3.80%	2.6[a]
Li_2S@Graphene	Li, CS_2 at 650 °C[45]	50–100 nm	C/10	805	200	0.12%	2.74
Li_2S@PC	LiH, CS_2 at 250 °C[48]	5–15 nm	C/2	716	300	0.18%	negligible
Li_2S@PC-CNT				1017	300	0.14%	negligible
Li_2S-CB	ball-milled Li_2SO_4, CO at 820 °C[51]	50–100 nm	C/10	943	50	0.62%	3.2
Li_2S@C	spray dry Li_2SO_4, RF at 820 °C[52]	10 nm	C/10	750			3.6
Li_2S@C-CNT			C/10	1100	200	0.29%	3.2
Li_2S@PC@CNF/CNF	freeze-dry Li_2SO_4, glucose, BC at 1000 °C[53]	~5 nm	C/5	700	400	0.07%	3.2
Li_2S/C fiber	electrospin $(LiSC_2H_4)_2$NMe, PVP at 700 °C[54]	~10 nm	C/20	870	100	0.43%	2.74[a]

[a]Overpotential not directly reported; data obtained from the CV curve.

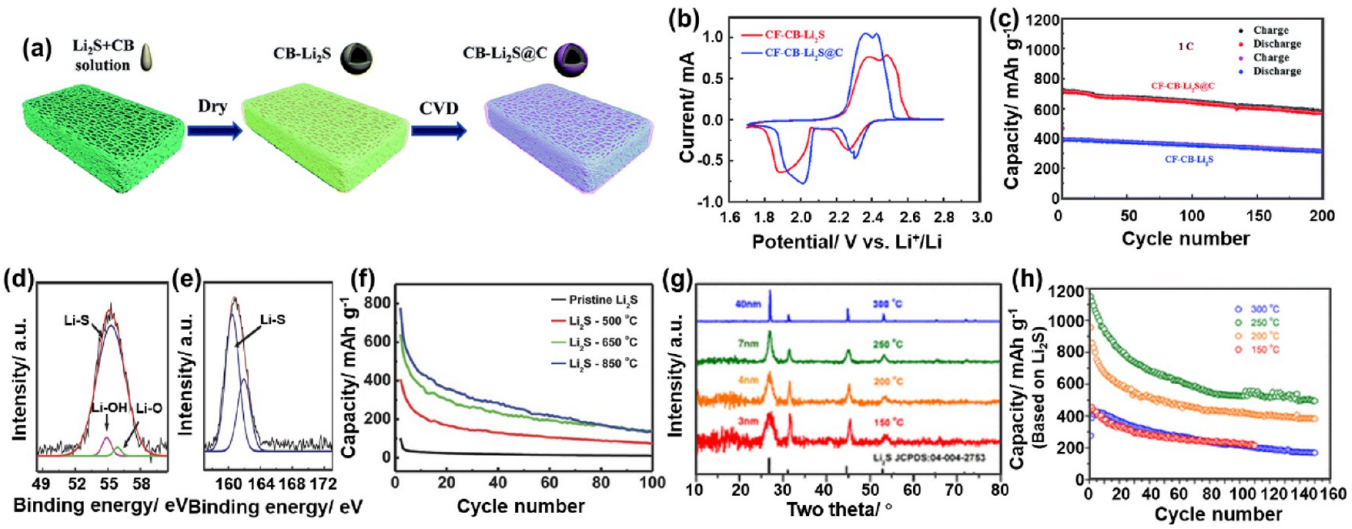

Figure 9. (a) Fabrication process for Li_2S@C from the Li_2S+CB solution, followed by carbon deposition via CVD, and evidence of (b) lowered overpotential and polarization, and (c) higher capacity and improved cycle stability as compared to Li_2S without a carbon coating. Adapted with permission from ref 55. Copyright 2017 Royal Society of Chemistry. XPS spectra of Li_2S (d) before and (e) after heating at 850 °C, showing the loss of LiOH, and (f) electrochemical performance of Li_2S after heating, showing improved capacity and cycle stability. Adapted with permission from ref 56. Copyright 2015 Wiley. (g) XRD pattern and Scherrer analysis of particle size after annealing at different temperatures and (h) their capacity and cycling stability comparison. Adapted with permission from ref 47. Copyright 2019 American Chemical Society.

nanoparticles below a threshold of 100 nm in size to achieve high sulfur utilization and suppress the first charge overpotential, summarized by the improved performance shown in Table 2. Further studies then found the use of liquid-phase synthesis to reprocess commercial Li_2S or lithiate sulfur nanoparticles with lithium-rich chemical solutions, allowing the nucleation of high-performance nanoparticles in the sub-100 nm size range. However, there is also a demand for atmospherically stable precursors to allow safe and scalable production of electrodes; thus recent investigations have turned to looking for novel facile synthesis methods. Notable improvements come from the carbothermic reduction of stable lithium salts; however, most new synthesis methods face the similar challenge of being unable to suppress the high

https://doi.org/10.1021/acsomega.2c05477
ACS Omega 2022, 7, 40682–40700

activation overpotential present in the first charge cycle as effectively, as compared to the methods involving the volatile precursors through gas/liquid-phase reactions. This issue regarding activation overpotential in cathodes obtained from safer methods such as carbothermic reaction requires further investigation for the new methods to be competitive in the realm concerning reaction kinetics and efficiency. It is however also evident from Table 2 that utilizing other strategies complementing the synthesis of nanosized particles can lead to further improvements, which will be discussed in the following section.

4.1.3. Confinement of Li_2S Cathode: From Li_2S to Substrates. 4.1.3.1. Confinement of Li_2S Particles. There are two interfaces that contribute to the high first charge overpotential of Li_2S cathodes: first, with the current collector and conductive elements that form the electrode with Li_2S, and, second, with the electrolyte. Well-engineered interfaces can enhance the charge transfer kinetics by facilitating the movement of electrons between the cathode material and the current collector, and the diffusion of Li^+ ions from the cathode to the electrolyte. Although the use of nanoparticles can significantly reduce the length of electron transfer and ion diffusion, a good contact with the current collector is still required to facilitate proper function. Beyond reducing the size of the commercial Li_2S particles, further treatment can be done to enhance the performance of the electrode. For example, carbon can be deposited uniformly onto the electrode via chemical vapor deposition (CVD) to form a Li_2S@carbon composite, which has been shown to enhance the reaction kinetics to not only lower the first charge overpotential, but also enhance the rate capability during he charge cycles. Furthermore, the carbon coating confines the active material, which can physically suppress the formation of long-chain LiPSs and their diffusion. Wang et al. have demonstrated this by comparing Li_2S particles with and without carbon coating via CVD (Figure 9a), showing a lower reduction potential and higher discharge capacity of 943 mAh g^{-1}, as compared to 601 mAh g^{-1} of its noncoated counterpart. Capacity retention is also notably increased to 72% after 100 cycles, as compared to 64% in its noncoated counterpart (Figure 9b,c).[55] The deposition of carbon can also be done prior to the complete synthesis of the Li_2S particles, where Chen et al. produced Li@C particles by plasma sparking lithium in CH_4 under an argon environment, and then sulfurizing it with sulfur vapor. The resultant cathode material had a negligible first charge overpotential, a high initial capacity of 1163 mAh g^{-1}, close to that of the theoretical limit, and a high capacity retention of 954 mAh g^{-1} after 100 cycles at 0.1 C, or 80% retention after 200 cycles at 5 C, a stark improvement in comparison to prior studies and also within the study's comparison group without the treatment.[57] This demonstrates the clear advantages of introducing carbon coating and its agreeability with its theoretical benefits. There are also other methods aimed to generate a carbon layer over the nanoparticles in a one-step process. For example, Tan et al. sulfurized lithium using CS_2 gas while making use of the carbon content to generate 10−20 layers of graphene over the particles, albeit with a much more violent combustion reaction. The graphene layers enabled suppression of overpotential to ∼2.7 V, and a capacity of over 600 mAh g^{-1} after 200 cycles.[45] Besides introducing carbon through high-energy reactions from the gas phase, polymers could act as carbon sources during the liquid-phase synthesis of Li_2S particles as well. Many synthesis methods involve controlling Li_2S particle growth with polymer encapsulation, or suspension within resin for additive manufacturing.[58] Chen et al. encapsulated ball-milled Li_2S/carbon black (CB) with PVP/pyrrole, and created a N-doped carbon shell after calcination with pyrrole as a nitrogen source.[33] Nitrogen has been shown to further enhance electron migration, thus increasing the electronic conductivity and performance of the fabricated Li_2S/CB@N-C material in a cell.[59]

In addition to the construction of conductive carbon shells, annealing also appears to contribute greatly to reducing the activation overpotential. Son et al. proposed that the surface decomposition of Li_2S forms a native layer of LiOH, which hinders Li^+ ion diffusion. This layer could be removed by annealing at 850 °C (Figure 9d,e), which could lower the activation potential barrier by as much as 0.4 V while significantly increasing the initial capacity as shown in Figure 9f.[56] It has also been suggested that dissolution processes during cathode fabrication can cause Li_2S to form electrochemically inactive compounds, such as $Li_2S{\cdot}CH_3CH_2OH$ with ethanol, which annealing at 200 °C proves to be sufficient to remove.[34] Zhao et al. further demonstrated the benefits by doing a comparison between the annealing temperature, finding 250 °C to be the optimum temperature for the removal of Li_2S−ethanol complexes, greatly enhancing the capacity to 98.5% of the Li_2S theoretical value along with a significant improvement in cycling stability (Figure 9h). This study also exposed the negative effects of the high-temperature processes, where annealing at 300 °C was shown to detrimentally affect the cell performance, likely due to particle growth and coalescence at high temperature as evidenced by Scherrer analysis of XRD patterns as shown in Figure 9g.[47]

Treatment of the nanoparticle surfaces has proved to be crucial in enhancing the performance of the Li_2S cathodes, as they govern the transfer of charge and ions at the interface. Carbon is shown to be an effective medium to interface Li_2S and the other cell components as a coating layer, while the formation of the LiOH native layer or other electrochemically inactive complexes can act in the electrode's detriment. The carbon coating process can sometimes render the annealing step redundant, as processes such as pyrolysis during the synthesis of Li_2S particles already make use of high temperatures. However, it remains important to beware of the potential interaction between Li_2S and its solvents that can occur during any synthesis step, and also exercise control over the particle growth and coalescence that comes with the use of high temperatures.

4.1.3.2. Confinement with Structured Hosts. An appropriate substrate can be used to boost the performance of the Li_2S cathode beyond what treatment on the particles itself can achieve. A good Li_2S host requires good conductivity for efficient charge transfer to the Li_2S, as well as adequate porosity to both contain the Li_2S and allow for sufficient electrolyte infiltration. Porous networks also have the additional benefit of physically confining dissolved LiPSs, which contribute to improved cycle stability. Carbon is among the most commonly used by virtue of its high conductivity and atmospherically inert nature for ease of handling. Studies have shown the easy availability of several commercial products that provide a wide variety of carbon allotropes for varying application methods,[60,62,63] with mesoporous allotropes being typically highly desired. For example, Liu et al. fabricated a composite mix of GO, CNT, and Li_2S, which was subsequently ball-milled with polyaniline (PANI) and then carbonized to

https://doi.org/10.1021/acsomega.2c05477
ACS Omega 2022, 7, 40682−40700

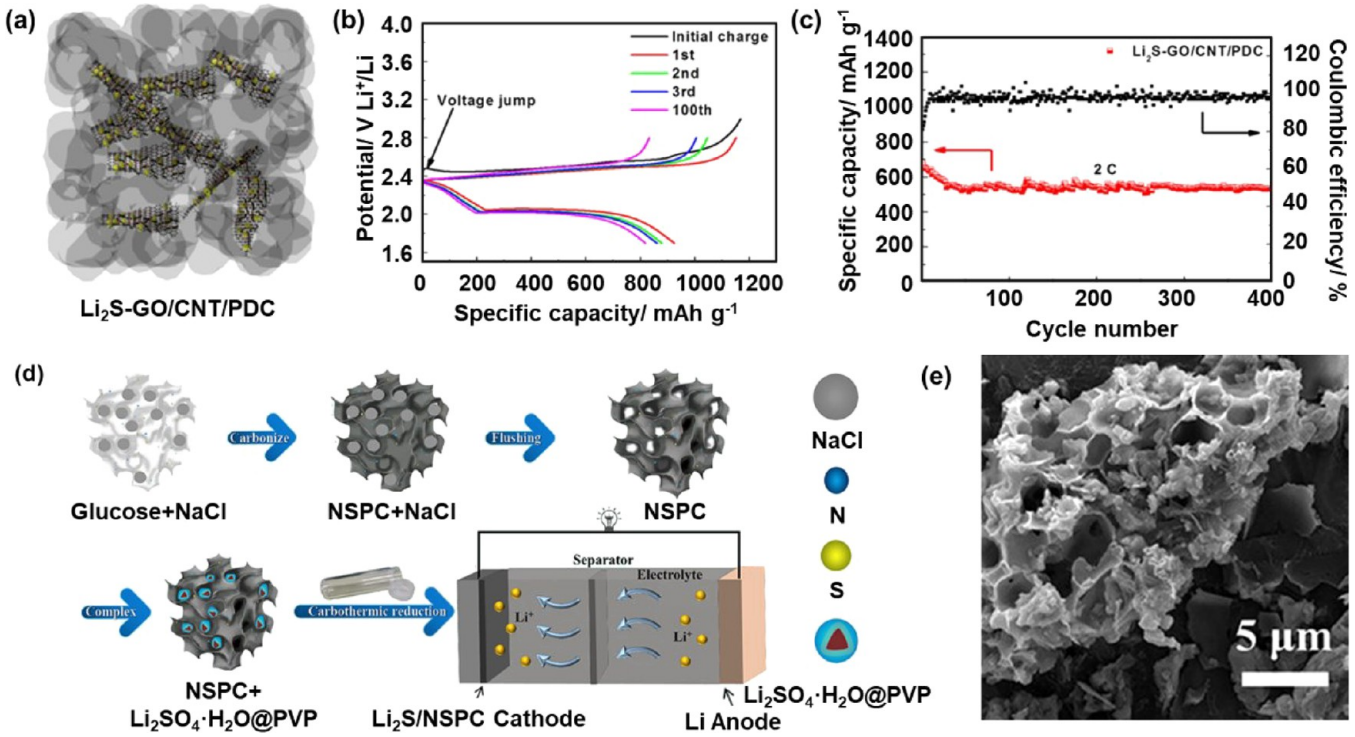

Figure 10. (a) Schematic of graphene oxide-anchored Li_2S hierarchically embedded in CNTs and PANI-derived carbon, resulting in (b) near complete elimination of the first charge overpotential and (c) excellent cycle stability. Adapted with permission from ref 60. Copyright 2020 American Chemical Society. (d) Illustration of the synthesis method of honeycomb porous carbon scaffold and (e) the resultant structure with Li_2S. Adapted with permission from ref 61. Copyright 2021 American Chemical Society.

form a heterostructure matrix as illustrated in Figure 10a. The PANI-derived carbon (PDC) matrix produced a superior pore volume, surface area, and a well-tuned pore size distribution at 3.5 nm, offering sufficient active sites for reaction and immobilization of LiPSs. Electrochemical testing revealed that this composite matrix was able to suppress the first charge to ∼2.5 V, nearly eliminating the overpotential as compared to that at 2.8 V without PDC, and delivered a high specific capacity of 925 mAh g^{-1} and excellent cycling ability, which remained stable over 400 cycles as shown in Figure 10b,c.[60] Composites with noncarbon porous matrixes have also been explored. For example, Kaiser et al. introduced Li_2S-MWCNT nanocomposites into a 3D nickel foam substrate through capillary action, aiming to free the electrode fabrication process from the use of polymer binders that may act as potential insulators and achieve higher active material loading. The Ni-foam matrix provided a multitude of beneficial functionalities, including acting as a highly conductive current collector and restricting SEI thickness, while the MWCNTs helped interface Li_2S with the functional matrix while offering physical confinement. The resulting cathode provided an initial capacity of as high as 1146 mAh g^{-1}, with an activation potential of 2.5 V. The cyclability was however lacking, retaining 49% after 100 cycles.[63]

Other novel methods to synthesize host structures have also been investigated, and the desired nanostructures can be derived from a variety of sources. For example, Li et al. fabricated electrodes by freeze-drying BC hydrogel with a glucose and Li_2SO_4 mixture. The subsequent carbothermal reaction of the mixture resulted in a ferroconcrete-like structure of interweaving carbon nanofibers with interconnecting porous carbon material derived from the glucose. The composite carbon structure served as an excellent charge conductor and suppressed LiPS formation effectively, with the resulting electrode retaining 71% of its initial capacity after 400 cycles. However, the first charge potential was fairly high at more than 3.5 V.[53] He et al. experimented with metal−organic frameworks (MOFs), generating C−Co−N porous frameworks through carbonizing ZIF-67 and infiltrating it with Li_2S in anhydrous ethanol solution. The highly crystalline 3D porous carbon matrix derived from the MOF offered physical confinement and adsorption of LiPS, effectively inhibiting the shuttling effect. The electrode was shown with a high cycling stability, retaining 81.7% of the initial capacity at 929 mAh g^{-1} even after 300 cycles, along with near complete elimination of the first charge overpotential.[64] Other than being inspired by the existing structures and to directly convert them into conductive networks with methods such as pyrolysis, an alternative strategy involved using existing structures as a scaffold instead. Yu et al. synthesized a highly porous structure from the freeze-dried water mixture of NaCl salt and glucose. After pyrolyzing the glucose into a N/S-doped carbon scaffold, the authors washed away the salt infill, leaving behind a highly porous interconnected honeycomb-like structure as illustrated in Figure 10d, which was finally used to host Li_2S derived from Li_2SO_4 solution. The final product (Figure 10e) demonstrated a negligible first charge overpotential of 2.4 V, a high discharge capacity of 1036 mAh g^{-1}, and an impressive cycling stability with 82.3% capacity retention after 100 cycles.[61]

These structures are able to provide several of the desired physical properties of a substrate, the continuous conductive channels of high surface area, and numerous Li_2S hosting sites with a pore size that limits LiPS formation and diffusion. By combining nanostructuring and effective functional substrates,

https://doi.org/10.1021/acsomega.2c05477
ACS Omega 2022, 7, 40682−40700

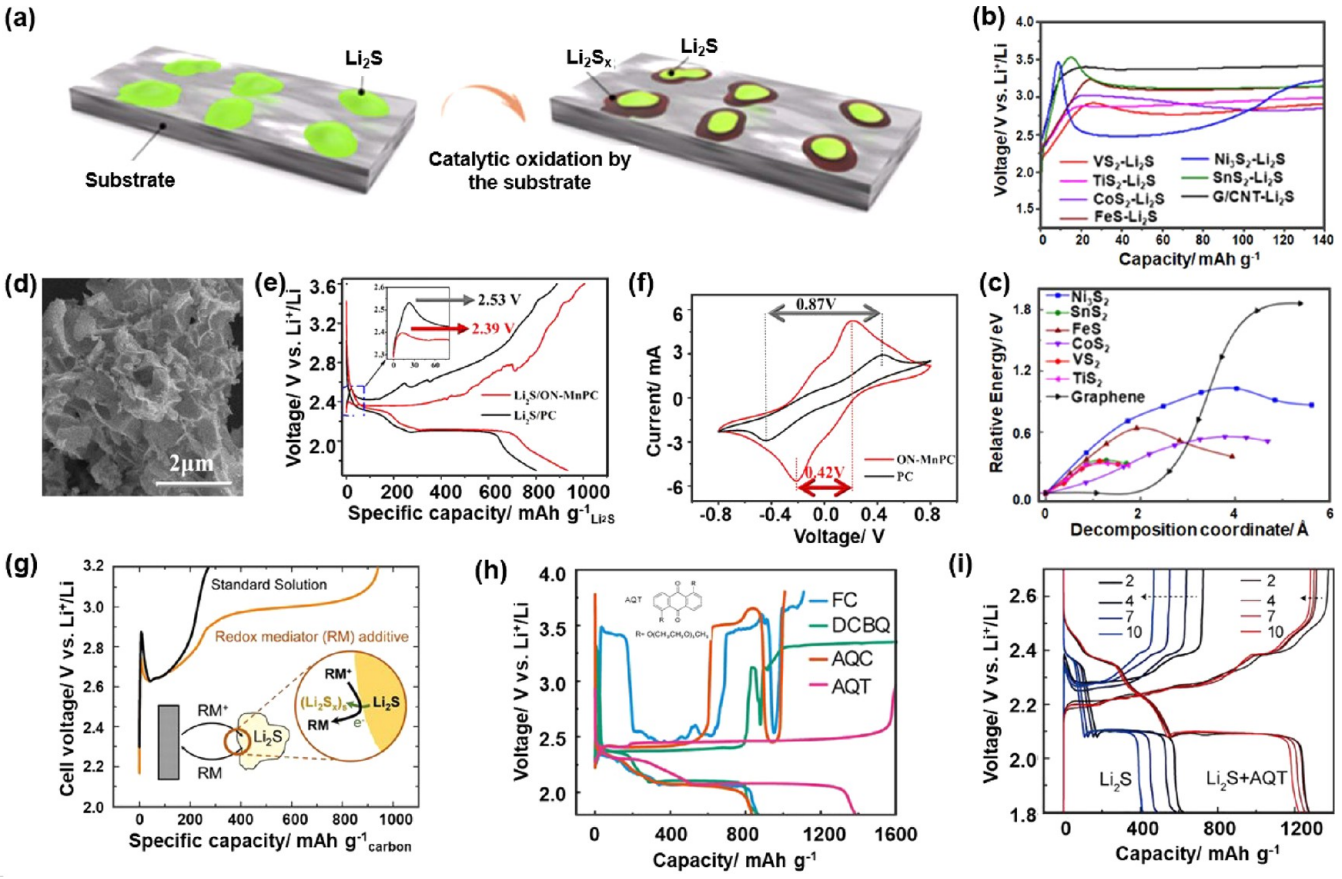

Figure 11. (a) Illustration of Li_2S decomposition on the catalytic substrate. Adapted with permission from ref 74. Creative Commons License (CC BY-NC-ND 4.0). (b) First charge overpotential of Li_2S batteries with various transition metal sulfide catalysts and (c) the decomposition barrier of Li_2S on the catalysts. Adapted with permission from ref 74. Creative Commons License (CC BY-NC-ND 4.0). (d) SEM image of Li_2S-infused Mn, O, and N catalyst on a honeycomb carbon support, showing (e) a reduced first charge overpotential and (f) a lowered charge/discharge polarization. Adapted with permission from ref 75. Copyright 2021 American Chemical Society. (g) Illustration of the mechanism of a redox mediator in Li_2S cathodes. Adapted with permission from ref 76. Copyright 2014 American Chemical Society. (h) Substantially reduced first charge overpotential and improved sulfur utilization of the AQT mediator (inset: AQT molecule) as compared to other mediators, and as compared to (i) pure Li_2S. Adapted with permission from ref 77. Copyright 2019 Elsevier.

the first charge potential can be reduced to near elimination, along with inhibition of the shuttling effect to allow capacity retention above 80% over 400 cycles.

4.2. Enhanced Interaction with Electrolyte – The Other Cathode Interface. Other than the substrate, the other interface that the cathode material interacts with is the electrolyte. The electrolyte serves as a medium for ion transportation, and in the case of a Li–S system, it also takes an active role in facilitating the conversion reaction between Li_2S and S_8 due to the presence of LiPS species. Their presence brings about various boons and banes to the cell's function. On the one hand, they promote the oxidation of Li_2S, thus reducing the reaction overpotential, and also allow for effective capacity utilization through their dissolution in the liquid phase. On the other hand, the associated shuttle effect brings about parasitic effects that corrode the anode, and lower the Coulombic efficiency and capacity decay from sulfur loss.[65] While it is a complex system that requires more exploration, Li_2S cathodes can leverage on current advances regarding electrolytes applicable in a traditional sulfur cathode LSB; however, extra consideration has to be made due to the presence of the first charge overpotential. This section details the ideal goal of tuning the solvent, salt, and additives, which form the electrolyte, showing the important functionality of the electrolyte in a Li_2S cathode LSB, and discuss the challenges and necessity to balance the benefits against the undesirable side effects.

While solvents can vary from each other in many parameters, their molecular polarity and Lewis basicity are key to their ability to coordinate with the acidic Li^+ ion, and thus how well they may dissolve LiPS species. Experiments reveal that a solvent's ability to dissolve LiPSs positively correlates with the quantified measures of dielectric constant and donor numbers, such as dimethyl sulfoxide (DMSO) that lies on the higher end of the spectrum exhibiting high LiPS solubility, and hydrofluoroethers (HFE) being on the other end. Commonly used solvents such as glymes, DOL, and DME moderately dissolve LiPSs. They are used to balance the solubility to utilize the advantages of enabling LiPS dissolution, without the need to be overly concerned with the parasitic issues from the shuttle effect. Su et al. further explored alternative solvent mixtures such as methyl *tert*-butyl ether (MtBE), tetrahydrofuran (THF), etc., to tune the electrolyte's solvating abilities to study the shuttling effect. In place of the typically used 1:1 DOL:DME solvent, 1:1 DOL:MtBE showed a stark increase in Coulombic efficiency and cycling stability, due to MtBE's low solvating ability, inhibiting LiPS dissolution and subsequent side reactions.[66] In the case of Li_2S cathodes, the dissociation

https://doi.org/10.1021/acsomega.2c05477
ACS Omega 2022, 7, 40682–40700

of the strong bond in Li_2S and its high overpotential precedes the formation of LiPSs, and this solid−liquid conversion is the limiting step to achieving higher performance.[67] Hence, the first charge is unable to benefit from dissolved LiPSs as liquid-phase redox mediators, resulting in the high overpotential. Liang et al. explored the use of trace ethanol, which Li_2S is highly soluble in, as a part of the solvent. This electrolyte design allowed the rate-limiting first step to benefit from the liquid-phase reaction, and effectively reduced the first charge overpotential by 0.8 V with 500 ppm ethanol.[68]

While existing solvents have been able to support the function of high-performance Li_2S cathodes, it should also be noted that current studies may often employ excessive electrolyte in favor of exploring other facets of improvement strategies. This however conceals some challenges that have to be faced to reach a high specific capacity at a cell level, in that a low electrolyte to active material ratio is required for further advancement.[69] While such lean electrolyte conditions are more desirable, they typically necessitate the use of highly LiPS-solvating solvents to facilitate ion transfer, which brings about the challenge of combating the shuttle effect. The salt contributes to the remaining bulk of the electrolyte's function, which can be added to fine-tune the intermolecular interaction between the solvent and LiPS to reach a desired solubility level. This is by virtue of the coordination effect, where anion ligands can be introduced to form complexes and promote dissolution, and also the use of the common ion effect, where the high concentration of Li^+ ion provided by the supporting salt can limit further dissolution of LiPS into the limited solvent. Pang et al. demonstrated how manipulating the salt to solvent ratio can yield desirable effects. With a high amount of lithium bis(trifluoromethanesulfonyl)imide (LiTFSI) salt in a diglyme (G2) solvent at 0.8:1 ratio, the solubility of LiPS was reduced due to there being limited uncoordinated oxygen moieties available. The relative abundance of LiTFSI salt forms a highly coordinated 3D network with the G2 molecule chains, reportedly forming a film-like layer that interacts with the cathode in a quasi-solid reaction, achieving a relatively high capacity retention of 83% after 100 cycles in a Li−S system.[70] It is also important to note the synergy between the solvent and salt, as demonstrated by Pang et al. in using other glymes such as G1, G3, and G4 instead of G2, where there appears to be higher level of free oxygen sites to facilitate LiPS dissolution due to weaker coordination between the molecules, or the extended glyme chain's oxygen moieties providing increased solvent activity.[70]

The conscious design and combination of electrolyte components can not only simply serve as the ion transport medium, but also provides extra functionality due to its interaction with LiPS, thus heavily impacting the reaction path during the conversion between Li_2S and S_8. Other methods can also be applied to augment the reaction pathway, importantly additives that can serve a function similar to that of LiPS in mediating the conversion, without the negative side effects that stem from polysulfide shuttling.

4.3. Kinetic Promotors: Catalytic/Mediating Additives. The aforementioned methods to improve Li_2S cathode performance act mostly on the physical interactions between various interfaces and the active material, ranging from reducing the charge diffusion length, controlling the contact area and confinement volume, and altering the method of interfacing through controlling the dissolution of various lithium and sulfur compounds present throughout the reaction pathway. The cell's performance may further be augmenting the chemical reaction itself with the introduction of catalysts and mediators,[71] which can be introduced to the substrate and/or the electrolyte, cooperatively enhancing the conversion kinetics and capacity utilization of Li_2S (Figure 11a). Rapid S/Li_2S conversion can also improve the cell cyclability by promoting direct solid−solid conversion and reducing the lifetime of the soluble LiPSs, inhibiting the shuttle effect, which nonpolar carbon hosts are prone to.[72,73]

Various transition metals and their compounds have been studied and used as catalysts. Zhou et al. demonstrated the catalytic effect of several transition metal sulfides on the activation barrier of Li_2S, with VS_2, TiS_2, CoS_2, and FeS all showing substantially reduced first-charge overpotentials as compared to carbon, while Ni_3S_2 and SnS_2 did not (Figure 11b).[74] The mechanism was elucidated through density functional theory (DFT) simulations, which showed reduced Li_2S decomposition barriers for the V, Ti, Co, Fe, and Sn sulfides due to stabilization of the Li-ion and LiPS decomposition products through strong coordination with the substrate (Figure 11c). The importance of good electronic conductivity in an effective catalyst was also illustrated with the high overpotential of SnS_2 despite the low decomposition barrier, which was attributed to its low conductivity. In addition, as the decomposition barrier is associated with LiPS coordination with the substrate, the sulfides with higher catalytic activity also demonstrated significantly improved cathode cycle stability. Yuan et al. conducted a similar investigation on the transition metal phosphides Ni_2P, Co_2P, and Fe_2P, showing a catalytic mechanism similar to that of the sulfides. Through DFT simulations, all three phosphides demonstrated strong coordination with Li_2S and substantially lower decomposition energies as compared to both pristine and N-doped carbon, leading to low first charge overpotentials of less than 2.6 V and improved cycle stability.[78] This mechanism was likewise observed in an oxide, $LiTiO_2$, which showed near complete elimination of the first charge overpotential and an outstanding cycle stability of just ∼3% capacity loss after 200 cycles, associated with the strong coordination between $LiTiO_2$ and Li_2S, as well as the longer chain polysulfides.[79]

Transition metals exhibit catalytic activity as single atoms as well. Han et al. modeled the interactions between the Li_2S clusters and the 3d transition metals from Sc through to Cu, where the metal atoms were supported on a carbon substrate through coordination to four nitrogen atoms.[80] The interaction strength was found to be smaller for the lower atomic number transition metals such as Ti and V, due to less filled antibonding states resulting in more effective d−p orbital hybridization between the transition metal and Li_2S. The strength of the bond between the transition metal atom and the Li_2S cluster was also found to be inversely correlated with that of the Li−S bonds within the cluster, leading to decreased Li_2S delithiation energy barriers. Although the Li_2S first charge overpotentials were not measured experimentally, the simulation results showed that all of the 3d-transition metal atoms from Sc to Co demonstrate lower Li_2S decomposition energy barriers than does carbon, and thus have the potential to be used as catalysts. Experimental evidence is nonetheless available from other studies. For example, Yu et al. synthesized a honeycomb-like carbon structure via a glucose−salt mixture method, introducing atomically dispersed manganese with $Mn(NO_3)_2$ salt in tandem with $(NH_3OH)Cl$. The method

https://doi.org/10.1021/acsomega.2c05477
ACS Omega 2022, 7, 40682−40700

created a functional carbon matrix embedded with catalytic Mn atoms coordinated with O and N (Figure 11d).[75] The electrode showed a low first charge overpotential of 2.4 V, as well as significantly lower charge/discharge polarization and higher sulfur utilization as compared to a cathode without catalysts (Figure 11e,f). Another example involved the use of Co−C nanocages encapsulated by closely packed MXene shells, where the Co was similarly found to both strongly adsorb LiPSs and reduce the energy barrier for Li_2S conversion.[81] As a result, the assembled cathode exhibited near complete elimination of the first charge overpotential and a sulfur utilization exceeding 90%. Cycle stability was also excellent, due to both LiPS adsorption by the catalyst and confinement by the MXene shell.

Nonmetallic heteroatom dopants can also be introduced onto carbon frameworks by carbonizing polymers that contain the desired element. Nitrogen, from polymer sources such as PVP,[33] is a common dopant and has been shown to improve the cathode performance by enhancing the matrix conductivity,[32] although direct catalytic effect is rarely demonstrated. That is achieved instead by non-nitrogen heteroatoms such as fluorine[82] or phosphorus,[83] likewise introduced with the dopant-containing polymers PVDF and P-doped PANI respectively. In both cases, the catalytic mechanism was again attributed to strong interaction between the heteroatoms and Li_2S and LiPSs and resulted in significant reductions in the first charge overpotentials and improved capacity retention after cycling as compared to the control frameworks without catalysts.

Redox mediators are able to enhance the conversion reaction in a different manner. Typically being dissolved species, mediators are first oxidized at a conductive site on the electrode, and in turn oxidize the Li_2S active material after diffusing to it (Figure 11g). This reduces the activation barrier as the mediated charge transfer process occurs more easily than direct charge transfer to insulating Li_2S. For example, Meini et al. investigated the effect of several potential mediators, including LiI and various metallocenes, and found that a redox potential higher than that of Li_2S was required for there to be a driving force for oxidation of Li_2S by the mediator.[76] As a result, LiI and ferrocenes, with redox potentials higher than Li_2S, exhibited higher sulfur utilization and lower first charge overpotentials than Cr- and Co-based metallocenes, with low redox potentials. Other mediators that have been investigated include the popular I/I^{3-} redox couple,[84] as well as quinone-based organic molecules.[77] Notably, a dimethoxyethoxy-substituted anthraquinone (AQT) was found to be able to reduce the first charge overpotential to less than 2.5 V even at a high charge rate of 0.5 C, along with sulfur utilization exceeding 80% and significantly improved cycle stability (Figure 11h,i).

Catalytic and mediating additives have been shown to be highly effective in reducing the first charge overpotential of Li_2S, and their often simultaneous ability to improve the cycle stability of the cathode addresses another key performance parameter of the cell. In addition, it is notable that Li_2S catalysts share the same general mechanism of Li_2S adsorption and PS stabilization with catalysts used in conventional LSBs,[85] suggesting that any material demonstrating catalytic effects in LSBs may also have the potential to reduce the Li_2S first charge overpotential. Such additives thus have excellent prospects to be used in tandem with other aforementioned strategies such as smaller Li_2S particles and physical confinement for high-performance Li_2S batteries.

5. SUMMARY AND PERSPECTIVES

With the high theoretical capacity and extremely low costs, Li−S batteries are undoubtedly among the most promising higher-performance batteries beyond lithium ion batteries. However, among the most challenging bottleneck faced by Li−S batteries is the poor cycling ability, where the conventional sulfur cathodes are plagued by numerous issues. One of the approaches that has been exploited is Li_2S cathodes, which can in part resolve these issues by allowing much higher processing temperatures, use of nonmetallic anodes, and with much lower volume expansion.

Nonetheless, for lithium sulfide batteries, the kinetic barriers leading to the high Li_2S first charge overpotential must be resolved, for which several different strategies have been identified, as detailed in the present overview. Reprocessing Li_2S by ball-milling or reprecipitation has been largely successful in reducing the particle sizes and the length of conductive pathways, with the latter method being able to nearly completely remove the first charge overpotential by sufficiently small particles. However, the processing of Li_2S remains overall difficult due to its air sensitivity, for which researchers have attempted several approaches, where one example is the in situ synthesis of Li_2S from stable precursors. While there have likewise been numerous successes to some extent, the frequent use of other air-sensitive or toxic precursors such as lithium metal and sulfide gases makes the synthesis process somewhat redundant. Li_2S synthesis through carbothermal reduction of lithium- and sulfur-containing salts appears to be highly promising, but continues to face challenges with achieving sufficiently small particle sizes to minimize the first charge overpotential, due to the typically high processing temperatures required.

Confinement of Li_2S within an appropriate conductive material, either by encapsulating Li_2S nanoparticles or infiltration of Li_2S into the structured host, has also shown some encouraging results. However, the nanoparticle encapsulation also likewise faces challenges with particle sizes, due to the processing temperature required to form the desired carbon shells. Ideal structured hosts, however, are typically substantially more difficult to synthesize and must be designed with sufficiently small and uniform pores to minimize the charge transfer lengths. Among the most promising results are those that have been shown with catalytic or mediating additives, which are able to achieve very low first charge overpotentials without strict requirements on the Li_2S particle sizes. In addition, the catalytic and mediating mechanisms can also simultaneously improve the cycle stability of the cathode, improving the overall cell performance as a whole for Li−S batteries.

While each of the individual strategies has shown its own set of benefits and also challenges, comprehensively addressing the kinetic barriers in Li_2S batteries would require their combinations. For example, preprocessing of commercial Li_2S materials or synthesis from stable precursors can and shall be combined with the appropriate structured, catalytic hosts to achieve the overall benefits. New synthesis methods should also take into account the scalability and production cost, as the eventual widespread adoption of Li_2S cathodes would require mass production at low cost, which is among the advantages of Li−S/sulfide batteries. As developments

https://doi.org/10.1021/acsomega.2c05477
ACS Omega 2022, 7, 40682−40700

continue along these paths, one shall see more commercial Li_2S batteries in the market, hopefully in the near future.

AUTHOR INFORMATION

Corresponding Authors

Jianguo Sun − *Department of Materials Science and Engineering, National University of Singapore, Singapore 117574, Singapore;* orcid.org/0000-0002-2222-2478; Email: sjg07@nus.edu.sg

John Wang − *Department of Materials Science and Engineering, National University of Singapore, Singapore 117574, Singapore; Institute of Materials Research and Engineering, A*STAR, Singapore 138634, Singapore;* orcid.org/0000-0001-6059-8962; Email: msewangj@nus.edu.sg

Authors

Lewis Kien Juen Ting − *Department of Materials Science and Engineering, National University of Singapore, Singapore 117574, Singapore*

Yulin Gao − *Department of Materials Science and Engineering, National University of Singapore, Singapore 117574, Singapore; ST Engineering Advanced Material Engineering Pte. Ltd., Singapore 619523, Singapore*

Haimei Wang − *Department of Materials Science and Engineering, National University of Singapore, Singapore 117574, Singapore*

Tuo Wang − *Department of Materials Science and Engineering, National University of Singapore, Singapore 117574, Singapore*

Complete contact information is available at: https://pubs.acs.org/10.1021/acsomega.2c05477

Author Contributions

‖L.K.J.T. and Y.G. contributed equally to this work.

Notes

The authors declare no competing financial interest.

ACKNOWLEDGMENTS

This work is supported by the MOE, Singapore Ministry of Education (Tier 1, A-8000186-01-00), research conducted at the National University of Singapore. L.K.J.T. acknowledges the NUS Engineering-Scholars Programme for their generous scholarship support. Y.G. acknowledges financial support by ST Engineering Advanced Material Engineering Pte. Ltd. and the Singapore Economic Development Board.

REFERENCES

(1) IEA. *Key World Energy Statistics 2021*; IEA: Paris, 2021.

(2) Gao, Y.; Pan, Z.; Sun, J.; Liu, Z.; Wang, J. High-Energy Batteries: Beyond Lithium-Ion and Their Long Road to Commercialisation. *Nano-Micro Lett.* **2022**, *14* (1), 94.

(3) Wu, G.; Sun, S.; Zhu, X.; Ma, Z.; Zhang, Y.; Bao, N. Microfluidic Fabrication of Hierarchical-Ordered ZIF-L(Zn)@$Ti_3C_2T_x$ Core-Sheath Fibers for High-Performance Asymmetric Supercapacitors. *Angew. Chem., Int. Ed.* **2022**, *61* (8), e202115559.

(4) Wu, G.; Ma, Z.; Wu, X.; Zhu, X.; Man, Z.; Lu, W.; Xu, J. Interfacial Polymetallic Oxides and Hierarchical Porous Core-Shell Fibres for High Energy-Density Electrochemical Supercapacitors. *Angew. Chem., Int. Ed.* **2022**, *61* (27), 1 DOI: 10.1002/anie.202203765.

(5) Sun, J.; Ye, H.; Oh, J. A. S.; Plewa, A.; Sun, Y.; Wu, T.; Sun, Q.; Zeng, K.; Lu, L. Elevating the Discharge Plateau of Prussian Blue Analogs through Low-Spin Fe Redox Induced Intercalation Pseudocapacitance. *Energy Storage Mater.* **2021**, *43*, 182−189.

(6) Chen, Y.; Wang, T.; Tian, H.; Su, D.; Zhang, Q.; Wang, G. Advances in Lithium-Sulfur Batteries: From Academic Research to Commercial Viability. *Adv. Mater.* **2021**, *33* (29), 2003666.

(7) Su, Y.-S.; Fu, Y.; Cochell, T.; Manthiram, A. A Strategic Approach to Recharging Lithium-Sulphur Batteries for Long Cycle Life. *Nat. Commun.* **2013**, *4* (1), 2985.

(8) Xu, W.; Wang, J.; Ding, F.; Chen, X.; Nasybulin, E.; Zhang, Y.; Zhang, J.-G. Lithium Metal Anodes for Rechargeable Batteries. *Energy Env. Sci.* **2014**, *7* (2), 513−537.

(9) Kang, W.; Deng, N.; Ju, J.; Li, Q.; Wu, D.; Ma, X.; Li, L.; Naebe, M.; Cheng, B. A Review of Recent Developments in Rechargeable Lithium-Sulfur Batteries. *Nanoscale* **2016**, *8* (37), 16541−16588.

(10) Zhang, K.; Qin, F.; Fang, J.; Li, Q.; Jia, M.; Lai, Y.; Zhang, Z.; Li, J. Nickel Foam as Interlayer to Improve the Performance of Lithium-Sulfur Battery. *J. Solid State Electrochem.* **2014**, *18* (4), 1025−1029.

(11) Liang, X.; Yun, J.; Wang, Y.; Xiang, H.; Sun, Y.; Feng, Y.; Yu, Y. A New High-Capacity and Safe Energy Storage System: Lithium-Ion Sulfur Batteries. *Nanoscale* **2019**, *11* (41), 19140−19157.

(12) Wang, D.-W.; Zeng, Q.; Zhou, G.; Yin, L.; Li, F.; Cheng, H.-M.; Gentle, I. R.; Lu, G. Q. M. Carbon-Sulfur Composites for Li-S Batteries: Status and Prospects. *J. Mater. Chem. A* **2013**, *1* (33), 9382.

(13) Xu, H.; Qie, L.; Manthiram, A. An Integrally-Designed, Flexible Polysulfide Host for High-Performance Lithium-Sulfur Batteries with Stabilized Lithium-Metal Anode. *Nano Energy* **2016**, *26*, 224−232.

(14) Cheon, S.-E.; Choi, S.-S.; Han, J.-S.; Choi, Y.-S.; Jung, B.-H.; Lim, H. S. Capacity Fading Mechanisms on Cycling a High-Capacity Secondary Sulfur Cathode. *J. Electrochem. Soc.* **2004**, *151* (12), A2067.

(15) Yang, Y.; Zheng, G.; Misra, S.; Nelson, J.; Toney, M. F.; Cui, Y. High-Capacity Micrometer-Sized Li_2S Particles as Cathode Materials for Advanced Rechargeable Lithium-Ion Batteries. *J. Am. Chem. Soc.* **2012**, *134* (37), 15387−15394.

(16) Ren, W.; Ma, W.; Zhang, S.; Tang, B. Recent Advances in Shuttle Effect Inhibition for Lithium Sulfur Batteries. *Energy Storage Mater.* **2019**, *23*, 707−732.

(17) Mikhaylik, Y. V.; Akridge, J. R. Polysulfide Shuttle Study in the Li/S Battery System. *J. Electrochem. Soc.* **2004**, *151* (11), A1969.

(18) Cheon, S.-E.; Ko, K.-S.; Cho, J.-H.; Kim, S.-W.; Chin, E.-Y.; Kim, H.-T. Rechargeable Lithium Sulfur Battery. *J. Electrochem. Soc.* **2003**, *150* (6), A800.

(19) Behzadirad, M.; Lavrova, O.; Busani, T. Demonstration of 99% Capacity Retention in Li/S Batteries with a Porous Hollow Carbon Cap Nanofiber-Graphene Structure through a Semi-Empirical Capacity Fading Model. *J. Mater. Chem. A* **2016**, *4* (20), 7830−7840.

(20) Li, Z.; Huang, J.; Yann Liaw, B.; Metzler, V.; Zhang, J. A Review of Lithium Deposition in Lithium-Ion and Lithium Metal Secondary Batteries. *J. Power Sources* **2014**, *254*, 168−182.

(21) Wu, F.; Magasinski, A.; Yushin, G. Nanoporous Li_2S and MWCNT-Linked Li_2S Powder Cathodes for Lithium-Sulfur and Lithium-Ion Battery Chemistries. *J. Mater. Chem. A* **2014**, *2* (17), 6064−6070.

(22) Wang, N.; Zhao, N.; Shi, C.; Liu, E.; He, C.; He, F.; Ma, L. In Situ Synthesized Li_2S@porous Carbon Cathode for Graphite/Li_2S Full Cells Using Ether-Based Electrolyte. *Electrochim. Acta* **2017**, *256*, 348−356.

(23) Ye, F.; Noh, H.; Lee, H.; Kim, H.-T. An Ultrahigh Capacity Graphite/Li_2S Battery with Holey-Li_2S Nanoarchitectures. *Adv. Sci.* **2018**, *5* (7), 1800139.

(24) Balach, J.; Jaumann, T.; Giebeler, L. Nanosized Li_2S-Based Cathodes Derived from MoS_2 for High-Energy Density Li-S Cells and Si-Li_2S Full Cells in Carbonate-Based Electrolyte. *Energy Storage Mater.* **2017**, *8*, 209−216.

(25) Hassoun, J.; Sun, Y.-K.; Scrosati, B. Rechargeable Lithium Sulfide Electrode for a Polymer Tin/Sulfur Lithium-Ion Battery. *J. Power Sources* **2011**, *196* (1), 343−348.

(26) Lee, S.-K.; Lee, Y. J.; Sun, Y.-K. Nanostructured Lithium Sulfide Materials for Lithium-Sulfur Batteries. *J. Power Sources* **2016**, *323*, 174−188.
(27) Zhang, L.; Sun, D.; Feng, J.; Cairns, E. J.; Guo, J. Revealing the Electrochemical Charging Mechanism of Nanosized Li_2S by in Situ and Operando X-Ray Absorption Spectroscopy. *Nano Lett.* **2017**, *17* (8), 5084−5091.
(28) Ye, H.; Li, M.; Liu, T.; Li, Y.; Lu, J. Activating Li_2S as the Lithium-Containing Cathode in Lithium-Sulfur Batteries. *ACS Energy Lett.* **2020**, *5* (7), 2234−2245.
(29) Cai, K.; Song, M.-K.; Cairns, E. J.; Zhang, Y. Nanostructured Li_2S-C Composites as Cathode Material for High-Energy Lithium/Sulfur Batteries. *Nano Lett.* **2012**, *12* (12), 6474−6479.
(30) Xiang, J.; Zhao, Y.; Wang, L.; Zha, C. The Presolvation Strategy of Li_2S Cathodes for Lithium-Sulfur Batteries: A Review. *J. Mater. Chem. A* **2022**, *10* (19), 10326−10341.
(31) Hu, C.; Chen, H.; Xie, Y.; Fang, L.; Fang, J.; Xu, J.; Zhao, H.; Zhang, J. Alleviating Polarization by Designing Ultrasmall Li_2S Nanocrystals Encapsulated in N-Rich Carbon as a Cathode Material for High-Capacity, Long-Life Li-S Batteries. *J. Mater. Chem. A* **2016**, *4* (47), 18284−18288.
(32) Chen, L.; Liu, Y.; Ashuri, M.; Liu, C.; Shaw, L. L. Li_2S Encapsulated by Nitrogen-Doped Carbon for Lithium Sulfur Batteries. *J. Mater. Chem. A* **2014**, *2* (42), 18026−18032.
(33) Chen, L.; Liu, Y.; Zhang, F.; Liu, C.; Shaw, L. L. PVP-Assisted Synthesis of Uniform Carbon Coated Li_2S/CB for High-Performance Lithium-Sulfur Batteries. *ACS Appl. Mater. Interfaces* **2015**, *7* (46), 25748−25756.
(34) Wang, C.; Wang, X.; Yang, Y.; Kushima, A.; Chen, J.; Huang, Y.; Li, J. Slurryless Li_2S/Reduced Graphene Oxide Cathode Paper for High-Performance Lithium Sulfur Battery. *Nano Lett.* **2015**, *15* (3), 1796−1802.
(35) Wu, M.; Cui, Y.; Fu, Y. Li_2S Nanocrystals Confined in Free-Standing Carbon Paper for High Performance Lithium-Sulfur Batteries. *ACS Appl. Mater. Interfaces* **2015**, *7* (38), 21479−21486.
(36) Capek, I. Radical Polymerization of Polar Unsaturated Monomers in Direct Microemulsion Systems. *Adv. Colloid Interface Sci.* **1999**, *80* (2), 85−149.
(37) Wu, F.; Lee, J. T.; Fan, F.; Nitta, N.; Kim, H.; Zhu, T.; Yushin, G. A Hierarchical Particle-Shell Architecture for Long-Term Cycle Stability of Li_2S Cathodes. *Adv. Mater.* **2015**, *27* (37), 5579−5586.
(38) Wu, F.; Kim, H.; Magasinski, A.; Lee, J. T.; Lin, H.-T.; Yushin, G. Harnessing Steric Separation of Freshly Nucleated Li_2S Nanoparticles for Bottom-Up Assembly of High-Performance Cathodes for Lithium-Sulfur and Lithium-Ion Batteries. *Adv. Energy Mater.* **2014**, *4* (11), 1400196.
(39) Hwa, Y.; Zhao, J.; Cairns, E. J. Lithium Sulfide (Li_2S)/Graphene Oxide Nanospheres with Conformal Carbon Coating as a High-Rate, Long-Life Cathode for Li/S Cells. *Nano Lett.* **2015**, *15* (5), 3479−3486.
(40) Yang, Y.; McDowell, M. T.; Jackson, A.; Cha, J. J.; Hong, S. S.; Cui, Y. New Nanostructured Li_2S/Silicon Rechargeable Battery with High Specific Energy. *Nano Lett.* **2010**, *10* (4), 1486−1491.
(41) Zhang, K.; Wang, L.; Hu, Z.; Cheng, F.; Chen, J. Ultrasmall Li2S Nanoparticles Anchored in Graphene Nanosheets for High-Energy Lithium-Ion Batteries. *Sci. Rep.* **2015**, *4* (1), 6467.
(42) Dressel, C. B.; Jha, H.; Eberle, A.-M.; Gasteiger, H. A.; Fässler, T. F. Electrochemical Performance of Lithium-Sulfur Batteries Based on a Sulfur Cathode Obtained by H_2S Gas Treatment of a Lithium Salt. *J. Power Sources* **2016**, *307*, 844−848.
(43) Hart, N.; Shi, J.; Zhang, J.; Fu, C.; Guo, J. Lithium Sulfide-Carbon Composites via Aerosol Spray Pyrolysis as Cathode Materials for Lithium-Sulfur Batteries. *Front. Chem.* **2018**, *6*, 476.
(44) Nava-Avendaño, J.; Nussbaum, M.; Veilleux, J. Thermal Plasma Synthesis of Li2S Nanoparticles for Application in Lithium-Sulfur Batteries. *Plasma Chem. Plasma Process.* **2021**, *41* (4), 1149−1167.
(45) Tan, G.; Xu, R.; Xing, Z.; Yuan, Y.; Lu, J.; Wen, J.; Liu, C.; Ma, L.; Zhan, C.; Liu, Q.; Wu, T.; Jian, Z.; Shahbazian-Yassar, R.; Ren, Y.; Miller, D. J.; Curtiss, L. A.; Ji, X.; Amine, K. Burning Lithium in CS_2 for High-Performing Compact Li_2S-Graphene Nanocapsules for Li-S Batteries. *Nat. Energy* **2017**, *2* (7), 17090.
(46) Li, X.; Zhao, Y.; Brennan, A.; McCeig, M.; Wolden, C. A.; Yang, Y. Reactive Precipitation of Anhydrous Alkali Sulfide Nanocrystals with Concomitant Abatement of Hydrogen Sulfide and Cogeneration of Hydrogen. *ChemSusChem* **2017**, *10* (14), 2904−2913.
(47) Zhao, Y.; Yang, Y.; Wolden, C. A. Scalable Synthesis of Size-Controlled Li_2S Nanocrystals for Next-Generation Battery Technologies. *ACS Appl. Energy Mater.* **2019**, *2* (3), 2246−2254.
(48) Liang, S.; Xia, Y.; Liang, C.; Gan, Y.; Huang, H.; Zhang, J.; Tao, X.; Sun, W.; Han, W.; Zhang, W. A Green and Facile Strategy for the Low-Temperature and Rapid Synthesis of Li_2S@PC-CNT Cathodes with High Li_2S Content for Advanced Li-S Batteries. *J. Mater. Chem. A* **2018**, *6* (21), 9906−9914.
(49) Karaseva, E. V.; Sheina, L. V.; Kolosnitsyn, V. S. Synthesis of Lithium Sulfide by Carbothermal Reduction of Lithium Sulfate with Petroleum Coke. *Russ. J. Appl. Chem.* **2021**, *94* (1), 1−8.
(50) Shi, J.; Zhang, J.; Zhao, Y.; Yan, Z.; Hart, N.; Guo, J. Synthesis of Li2S-Carbon Cathode Materials via Carbothermic Reduction of Li_2SO_4. *Front. Energy Res.* **2019**, *7*, 53.
(51) Kohl, M.; Brückner, J.; Bauer, I.; Althues, H.; Kaskel, S. Synthesis of Highly Electrochemically Active Li_2S Nanoparticles for Lithium-Sulfur-Batteries. *J. Mater. Chem. A* **2015**, *3* (31), 16307−16312.
(52) Chen, X.; Peng, L.; Yuan, L.; Zeng, R.; Xiang, J.; Chen, W.; Yuan, K.; Chen, J.; Huang, Y.; Xie, J. Facile Synthesis of Li_2S@C Composites as Cathode for Li-S Batteries. *J. Energy Chem.* **2019**, *37*, 111−116.
(53) Li, S.; Jiang, J.; Dong, Z.; Wu, J.; Cheng, Z.; Zhu, H.; Fan, Z.; Wang, Y.; Leng, D. Ferroconcrete-Inspired Construction of Self-Supporting Li_2S Cathode for High-Performance Lithium-Sulfur Batteries. *Microporous Mesoporous Mater.* **2020**, *293*, 109822.
(54) Brune, V.; Bohr, C.; Ludwig, T.; Wilhelm, M.; Hirt, S. D.; Fischer, T.; Wennig, S.; Oberschachtsiek, B.; Ichangi, A.; Mathur, S. A Novel Molecular Synthesis Route to Li_2S Loaded Carbon Fibers for Lithium-Sulfur Batteries. *J. Mater. Chem. A* **2022**, *10* (18), 9902−9910.
(55) Wang, D.; Xie, D.; Xia, X.; Zhang, X.; Tang, W.; Zhong, Y.; Wu, J.; Wang, X.; Tu, J. A 3D Conductive Network with High Loading Li_2S@C for High Performance Lithium-Sulfur Batteries. *J. Mater. Chem. A* **2017**, *5* (36), 19358−19363.
(56) Son, Y.; Lee, J.-S.; Son, Y.; Jang, J.-H.; Cho, J. Recent Advances in Lithium Sulfide Cathode Materials and Their Use in Lithium Sulfur Batteries. *Adv. Energy Mater.* **2015**, *5* (16), 1500110.
(57) Chen, C.; Li, D.; Gao, L.; Harks, P. P. R. M. L.; Eichel, R.-A.; Notten, P. H. L. Carbon-Coated Core-Shell Li_2S@C Nanocomposites as High Performance Cathode Materials for Lithium-Sulfur Batteries. *J. Mater. Chem. A* **2017**, *5* (4), 1428−1433.
(58) Saccone, M. A.; Greer, J. R. Understanding and Mitigating Mechanical Degradation in Lithium-Sulfur Batteries: Additive Manufacturing of Li_2S Composites and Nanomechanical Particle Compressions. *J. Mater. Res.* **2021**, *36* (18), 3656−3666.
(59) Song, J.; Xu, T.; Gordin, M. L.; Zhu, P.; Lv, D.; Jiang, Y.-B.; Chen, Y.; Duan, Y.; Wang, D. Nitrogen-Doped Mesoporous Carbon Promoted Chemical Adsorption of Sulfur and Fabrication of High-Areal-Capacity Sulfur Cathode with Exceptional Cycling Stability for Lithium-Sulfur Batteries. *Adv. Funct. Mater.* **2014**, *24* (9), 1243−1250.
(60) Liu, H.; Zeng, P.; Li, Y.; Yu, H.; Chen, M.; Jamil, S.; Miao, C.; Chen, G.; Liu, Q.-C.; Luo, Z.; Wang, X. Polyaniline-Derived Carbon Heterostructure as Redox Mediator of Li_2S Oxidation and Polysulfide Immobilizer for High-Performance Lithium-Sulfur Cathode. *ACS Sustain. Chem. Eng.* **2020**, *8* (44), 16659−16670.
(61) Yu, H.; Zeng, P.; Liu, H.; Zhou, X.; Guo, C.; Li, Y.; Liu, S.; Chen, M.; Guo, X.; Chang, B.; Wu, T.; Wang, X. Li_2S In Situ Grown on Three-Dimensional Porous Carbon Architecture with Electron/Ion Channels and Dual Active Sites as Cathodes of Li-S Batteries. *ACS Appl. Mater. Interfaces* **2021**, *13* (28), 32968−32977.

https://doi.org/10.1021/acsomega.2c05477
ACS Omega 2022, 7, 40682−40700

(62) Wang, D. H.; Xie, D.; Yang, T.; Zhong, Y.; Wang, X. L.; Xia, X. H.; Gu, C. D.; Tu, J. P. Conversion from Li_2SO_4 to Li_2S@C on Carbon Paper Matrix: A Novel Integrated Cathode for Lithium-Sulfur Batteries. *J. Power Sources* **2016**, *331*, 475−480.
(63) Kaiser, M. R.; Liang, X.; Liu, H.-K.; Dou, S.-X.; Wang, J.-Z. A Methodical Approach for Fabrication of Binder-Free Li_2S-C Composite Cathode with High Loading of Active Material for Li-S Battery. *Carbon* **2016**, *103*, 163−171.
(64) He, J.; Chen, Y.; Lv, W.; Wen, K.; Xu, C.; Zhang, W.; Li, Y.; Qin, W.; He, W. From Metal-Organic Framework to Li_2S@C-Co-N Nanoporous Architecture: A High-Capacity Cathode for Lithium-Sulfur Batteries. *ACS Nano* **2016**, *10* (12), 10981−10987.
(65) Liu, Y.; Elias, Y.; Meng, J.; Aurbach, D.; Zou, R.; Xia, D.; Pang, Q. Electrolyte Solutions Design for Lithium-Sulfur. *Batteries. Joule* **2021**, *5* (9), 2323−2364.
(66) Su, C.; He, M.; Amine, R.; Chen, Z.; Amine, K. The Relationship between the Relative Solvating Power of Electrolytes and Shuttling Effect of Lithium Polysulfides in Lithium-Sulfur Batteries. *Angew. Chem., Int. Ed.* **2018**, *57* (37), 12033−12036.
(67) Zhou, G.; Yang, A.; Gao, G.; Yu, X.; Xu, J.; Liu, C.; Ye, Y.; Pei, A.; Wu, Y.; Peng, Y.; Li, Y.; Liang, Z.; Liu, K.; Wang, L.-W.; Cui, Y. Supercooled Liquid Sulfur Maintained in Three-Dimensional Current Collector for High-Performance Li-S Batteries. *Sci. Adv.* **2020**, *6* (21), eaay5098.
(68) Liang, X.; Yun, J.; Xu, K.; Shi, P.; Sun, Y.; Chen, C.; Xiang, H. Trace Ethanol as an Efficient Electrolyte Additive to Reduce the Activation Voltage of the Li_2S Cathode in Lithium-Ion-Sulfur Batteries. *Chem. Commun.* **2019**, *55* (68), 10088−10091.
(69) Zhou, G.; Chen, H.; Cui, Y. Formulating Energy Density for Designing Practical Lithium-Sulfur Batteries. *Nat. Energy* **2022**, *7* (4), 312−319.
(70) Pang, Q.; Shyamsunder, A.; Narayanan, B.; Kwok, C. Y.; Curtiss, L. A.; Nazar, L. F. Tuning the Electrolyte Network Structure to Invoke Quasi-Solid State Sulfur Conversion and Suppress Lithium Dendrite Formation in Li-S Batteries. *Nat. Energy* **2018**, *3* (9), 783−791.
(71) Ye, H.; Sun, J.; Lim, X. F.; Zhao, Y.; Lee, J. Y. Mediator-Assisted Catalysis of Polysulfide Conversion for High-Loading Lithium-Sulfur Batteries Operating Under the Lean Electrolyte Condition. *Energy Storage Mater.* **2021**, *38*, 338−343.
(72) Shao, Q.; Xu, L.; Guo, D.; Su, Y.; Chen, J. Atomic Level Design of Single Iron Atom Embedded Mesoporous Hollow Carbon Spheres as Multi-Effect Nanoreactors for Advanced Lithium-Sulfur Batteries. *J. Mater. Chem. A* **2020**, *8* (45), 23772−23783.
(73) Zeng, P.; Liu, C.; Zhao, X.; Yuan, C.; Chen, Y.; Lin, H.; Zhang, L. Enhanced Catalytic Conversion of Polysulfides Using Bimetallic Co_7Fe_3 for High-Performance Lithium-Sulfur Batteries. *ACS Nano* **2020**, *14* (9), 11558−11569.
(74) Zhou, G.; Tian, H.; Jin, Y.; Tao, X.; Liu, B.; Zhang, R.; Seh, Z. W.; Zhuo, D.; Liu, Y.; Sun, J.; Zhao, J.; Zu, C.; Wu, D. S.; Zhang, Q.; Cui, Y. Catalytic Oxidation of Li_2S on the Surface of Metal Sulfides for Li−S Batteries. *Proc. Natl. Acad. Sci. U. S. A.* **2017**, *114* (5), 840−845.
(75) Yu, H.; Zeng, P.; Zhou, X.; Guo, C.; Liu, X.; Wang, K.; Guo, X.; Chang, B.; Chen, M.; Wang, X. Atomically Dispersed and O, N-Coordinated Mn-Based Catalyst for Promoting the Conversion of Polysulfides in Li_2S-Based Li-S Battery. *ACS Appl. Mater. Interfaces* **2021**, *13* (45), 54113−54123.
(76) Meini, S.; Elazari, R.; Rosenman, A.; Garsuch, A.; Aurbach, D. The Use of Redox Mediators for Enhancing Utilization of Li_2S Cathodes for Advanced Li-S Battery Systems. *J. Phys. Chem. Lett.* **2014**, *5* (5), 915−918.
(77) Tsao, Y.; Lee, M.; Miller, E. C.; Gao, G.; Park, J.; Chen, S.; Katsumata, T.; Tran, H.; Wang, L.-W.; Toney, M. F.; Cui, Y.; Bao, Z. Designing a Quinone-Based Redox Mediator to Facilitate Li_2S Oxidation in Li-S Batteries. *Joule* **2019**, *3* (3), 872−884.
(78) Yuan, H.; Chen, X.; Zhou, G.; Zhang, W.; Luo, J.; Huang, H.; Gan, Y.; Liang, C.; Xia, Y.; Zhang, J.; Wang, J.; Tao, X. Efficient Activation of Li_2S by Transition Metal Phosphides Nanoparticles for Highly Stable Lithium-Sulfur Batteries. *ACS Energy Lett.* **2017**, *2* (7), 1711−1719.
(79) Wu, F.; Pollard, T. P.; Zhao, E.; Xiao, Y.; Olguin, M.; Borodin, O.; Yushin, G. Layered $LiTiO_2$ for the Protection of Li_2S Cathodes against Dissolution: Mechanisms of the Remarkable Performance Boost. *Energy Environ. Sci.* **2018**, *11* (4), 807−817.
(80) Han, Z.; Zhao, S.; Xiao, J.; Zhong, X.; Sheng, J.; Lv, W.; Zhang, Q.; Zhou, G.; Cheng, H. Engineering *d-p* Orbital Hybridization in Single-Atom Metal-Embedded Three-Dimensional Electrodes for Li-S Batteries. *Adv. Mater.* **2021**, *33* (44), 2105947.
(81) Liu, Y.; Meng, X.; Wang, Z.; Qiu, J. A Li_2S-Based All-Solid-State Battery with High Energy and Superior Safety. *Sci. Adv.* **2022**, *8* (1), eabl8390.
(82) Zhang, J.; Xu, E.; Sun, Z.; Zhou, Y.; Shi, P.; Gao, Y.; Bao, Z.; Jiang, Y. Inverse Fabrication of Li_2S-Nanocrystals@Doped-Carbon Loaded on Woven Carbon Fibers to Spatial Structure Cathodes for High-Stable Lithium-Sulfur Batteries. *Small. Methods* **2020**, *4* (12), 2000463.
(83) Zhang, J.; Shi, Y.; Ding, Y.; Peng, L.; Zhang, W.; Yu, G. A Conductive Molecular Framework Derived Li_2S/N,P-Codoped Carbon Cathode for Advanced Lithium-Sulfur Batteries. *Adv. Energy Mater.* **2017**, *7* (14), 1602876.
(84) Liu, M.; Ren, Y. X.; Jiang, H. R.; Luo, C.; Kang, F. Y.; Zhao, T. S. An Efficient Li_2S-Based Lithium-Ion Sulfur Battery Realized by a Bifunctional Electrolyte Additive. *Nano Energy* **2017**, *40*, 240−247.
(85) Han, Z.; Gao, R.; Jia, Y.; Zhang, M.; Lao, Z.; Chen, B.; Zhang, Q.; Li, C.; Lv, W.; Zhou, G. Catalytic Effect in Li-S Batteries: From Band Theory to Practical Application. *Mater. Today* **2022**, *57*, 84−120.

https://doi.org/10.1021/acsomega.2c05477
ACS Omega 2022, 7, 40682−40700